ARL-PROP-R-177

AR-006-126






# DEPARTMENT OF DEFENCE

## DEFENCE SCIENCE AND TECHNOLOGY ORGANISATION

## AERONAUTICAL RESEARCH LABORATORY

MELBOURNE, VICTORIA

Propulsion Report 177

# AEROTHERMODYNAMIC DESIGN APPRAISAL OF NOISE SUPPRESSORS FOR F/A-18 ENGINE RUN-UP FACILITIES AT RAAF WILLIAMTOWN


by

S.A. Fisher and A.M. Abdel-Fattah



Approved for public release





OCTOBER 1990

AR-006-126

**DEPARTMENT OF DEFENCE**
**DEFENCE SCIENCE AND TECHNOLOGY ORGANISATION**
**AERONAUTICAL RESEARCH LABORATORY**

Propulsion Report 177

# AEROTHERMODYNAMIC DESIGN APPRAISAL OF NOISE SUPPRESSORS FOR F/A-18 ENGINE RUN-UP FACILITIES AT RAAF WILLIAMTOWN

by

S.A. Fisher and A.M. Abdel-Fattah

## SUMMARY

*Upgraded facilities for ground running of F404 engines in F/A-18 aircraft at RAAF Williamtown will feature air-cooled exhaust augmentors for noise suppression. Aerothermodynamic aspects of the augmentor designs were appraised in some detail, making use of isothermal scale model tests, ejector theory and available empirical data.*

*In initial design development, quantitative assessments were made of cooling flow pumping performance. Changes were recommended to improve the aerodynamic characteristics of the exhaust augmentors and eliminate high risk features, and the sizes of the augmentor ducts were significantly reduced. The model tests identified certain geometric features which were important for symmetry of the flow in the augmentor ducts and to pumping performance. Once modified accordingly, the designs displayed satisfactory aerodynamic behaviour, which was tolerant to both inlet asymmetries and reasonable levels of engine jet misalignment. The pumping performance was shown to exceed the design requirements.*




**POSTAL ADDRESS:** **Director, Aeronautical Research Laboratory**
**506 Lorimer Street, Fishermens Bend Victoria 3207**
**Australia**

# NOTATION

| | | |
|---|---|---|
| A | Local flow area | |
| $C_p$ | Specific heat at constant pressure | |
| d | Diameter of round primary augmentor tube | |
| H | Enthalpy | |
| h | Height of obround primary augmentor tube | |
| I | Momentum | |
| J | Steam thrust | |
| k | Pressure loss coefficient | |
| l | Length of primary augmentor tube | |
| M | Mach number | |
| m | Mass flow rate | |
| P | Static pressure | |
| $P_o$ | Total pressure | |
| R | Gas constant | |
| T | Total temperature | |
| w | Width of obround primary augmentor tube | |
| $\gamma$ | Ratio of specific heats | |
| $\mu$ | Augmentation ratio | m"/m' |
| $\nu$ | Augmentor area ratio | Main duct/Nozzle throat area |

Superscripts

| | |
|---|---|
| ' | Jet flow |
| " | Entrained flow |

Subscripts

| | |
|---|---|
| a | Ambient conditions |
| 1 | Entry plane of augmentor duct |
| 2 | Exit plane of augmentor duct |

# CONTENTS

# 1. INTRODUCTION

Facilities at RAAF Base Williamtown for extended ground running of F404 engines in F/A-18 aircraft are being upgraded, mainly to reduce noise emissions. Provision is to be made for running both uninstalled engines mounted on a test stand, and engines installed in aircraft, at up to full afterburning power.

For effective suppression of exhaust noise in jet engine run-up facilities, the high velocity exhaust jets must be enclosed and treated such that the engine and jet noise are absorbed, and the velocity of the final suppressor efflux is sufficiently low for its noise level to be acceptable. This can be most readily achieved with the introduction of water, but with attendant penalties which include high capital and operating costs, structural corrosion and environmental problems. Modern facilities are generally air-cooled, using exhaust augmentors to enclose the hot, high velocity jets and entrain atmospheric air for cooling and noise suppression.

Exhaust augmentors for afterburning engines are subject to very high levels of input energy flux, and require effective integration of aerothermodynamic, acoustic and structural design technologies for successful, long life operation. In particular, satisfactory internal aerodynamic performance and behaviour are critical to their operational effectiveness and durability. Not only must an augmentor pump sufficient cooling air to reduce the final mixed flow velocity and temperature to acceptable levels, but the flow within the augmentor must be stable, with no danger of direct impingement of uncooled exhaust gases on the duct walls. Any tendency towards instability or asymmetry of the internal flow may cause overheating, excessive aerodynamic loading and premature structural failure.

Responsibility for the design of the RAAF Williamtown exhaust augmentors rested with the architectural and acoustic design consultant, L.A. Challis and Associates Pty Ltd, contracted by the construction authority, Australian Construction Services (ACS) on behalf of RAAF. Aeronautical Research Laboratory (ARL) undertook an independent appraisal of aerothermodynamic design aspects, both in support of RAAF Facilities Branch and as a consultant to ACS. The outcomes of these ARL activities have been summarised in References 1 and 2, and are described more comprehensively in the present Report.

# 2. DESIGN DEVELOPMENT

## 2.1 Early Design Proposals

A number of facilities of the sort required are in service elsewhere, and installations are available commercially. A survey of such facilities[3] found that, whilst they are generally effective, a large range of durability problems have been experienced, apparently resulting from design and construction deficiencies. This, together with cost considerations and some perceived unique RAAF operational requirements, led to the adoption of an approach involving local design and construction.

For operational reasons separate, independent facilities were required for testing installed and uninstalled engines. Early design concepts[3] for the two facilities are shown in Figures 1 and 2. The augmentor designs were based on reinforced concrete ducts of square cross section, lined with modular, stainless steel-faced acoustic treatment. A deliberately conservative approach was adopted by the designer in the choice of generously sized augmentor ducts, to maximise the entrained cooling flow and minimise the possibility of hot jet impingement on the duct linings. Some issues of concern with these designs included:

- The asymmetrical secondary flow inlet arrangements, and their possible adverse effect on the symmetry of the downstream flow.

- The questionable practicality of close-coupling the engine exhaust nozzles to the augmentor inlets, and the effect of this on thrust measurement in the case of the uninstalled engine.

- The durability of the turning vanes at the foot of the exhaust stacks.

Following a review of RAAF requirements, the close-coupling arrangements were eliminated in new designs[4], permitting simpler inlet arrangements for the cooling air. These designs are shown in Figures 3 and 4. A "rectifier" system, consisting of stacked pipes, was added to the downstream end of the installed engine augmentor duct to alleviate the effect of asymmetrical operation of the twin engines, and to ease the operating environment of the turning vanes.

New technical concerns with these proposals were:

- The prospect of excessive air velocities around the rear of the aircraft in the installed engine facility, and the possible effects of the resultant wind forces on safety and convenience of operations.

- Depression in the uninstalled engine test enclosure, and the effect of this on engine thrust measurement.

The estimated construction costs also became a major issue, necessitating a review of several features of the designs, including the size of the augmentor ducts. To help with the resolution of these issues, a quantitative assessment was undertaken of the pumping performance of the augmentors, including comparison of different engine operating modes and assessment of the effect of duct size.

## 2.2 Estimation of Pumping Performance

### 2.2.1 Theoretical approach

Ejector theory using compressible flow relationships based on principles of conservation of mass, momentum and energy may be used to calculate rates of entrainment of cooling air in an augmentor duct. The basic theory uses one-dimensional flow relationships with no friction losses, treating the flow at the duct exit as fully mixed and uniform. Losses in various parts of the duct, such as the entrained (secondary) flow inlet system, the duct walls and the exhaust stack, may be

accounted for with appropriate pressure drop coefficients, and the effect of incomplete mixing between the jet and the entrained flow within the duct may also be accommodated if the non-uniform distributions of velocity, temperature and gas properties are known[5].

The simplified flow model adopted for the present exercise is shown in Figure 5. Departures from idealised conditions were accommodated by the application of two variable loss coefficients, $k_1$ and $k_2$, defined as follows:

$$k_1 = 2(P_a - P_1)/P_1\gamma_1 M_1^2 - 1$$

$$k_2 = 2(P_2 - P_a)/P_2\gamma_2 M_2^2$$

Notional pressure losses were thus imposed at the secondary flow inlet system and the augmentor duct exit, and it was implied that the effects of all losses, including wall friction, could be lumped into these two coefficients. The effect of incomplete mixing in the augmentor ducts was not expected to be sufficient to warrant specific treatment. According to experience[6,7], the pumping performance of installations of this type becomes relatively insensitive to augmentor duct length when the ratio of length to hydraulic diameter is greater than about 4; this suggests that the kinetic and thermal mixing which occurs downstream of 4 hydraulic diameters has little impact on the augmentation ratio. Evidence from model tests, described in Section 3 below, shows that kinetic mixing with isothermal flow is actually far from complete at 4 hydraulic diameters. However, as will be seen, the ultimate designs had length to hydraulic diameter ratios in excess of 6, dictated by acoustic considerations. Moreover, increased rates of mixing are known to occur in ejectors when the jet temperature differential is increased to the levels of present interest[5,8].

The relationships used in the theoretical treatment, referring to the flow stations in Figure 5, were as follows:

Conservation of Mass

$$m_2 = m_1' + m_1'' \qquad m = PAM\sqrt{[1 + (\gamma-1)M^2/2]\gamma/RT}$$

Conservation of Momentum

$$J_2 = J_1' + J_1'' \qquad J = PA(1 + \gamma M^2)$$

Conservation of Energy

$$H_2 = H_1' + H_1'' \qquad H = mC_pT$$

Pressure Balance

$$P_1'' = P_a/[1 + (1+k_1)\gamma_1''M_1''^2/2]$$

$$P_2 = P_a/[1 - k_2\gamma_2 M_2^2/2]$$

The solution of the equations and procedure for calculating augmentor performance are fully described in Reference 8.

2.2.2 Comparison of operating modes

Since the F/A-18 is a twin-engined aircraft, the installed engine test facility may have to accommodate either one operating engine, or two engines operating simultaneously. A limitation accepted by RAAF is the operation of only one of the two engines at any one time in the maximum afterburner (max A/B) mode, the other being either shut down or limited to idle power. The maximum power level at which two engines may be operated simultaneously is intermediate rated power (IRP), equivalent to maximum dry or military power.

To compare the loading on the installed engine augmentor for the above two cases (ie. one engine at max A/B or two engines at IRP), theoretical assessments were made of augmentor performance at both conditions. A simple comparison based on energy input suggests that a single engine at max A/B represents the more severe condition, since the total fuel flow to an engine at this power setting is almost four times that at IRP. To confirm this, augmentor performance was calculated for each case with four different combinations of the two loss coefficients, for an augmentor duct cross sectional area corresponding to the designs shown in Figures 3 and 4. The single engine, IRP case was also included. The high value of 2.5 assigned to the exit loss coefficient was chosen to ensure that the effect of relatively complex exhaust stack arrangements would be covered by the calculations. The figures used for air and fuel mass flow, exhaust temperature and pressure, nozzle configuration and exhaust gas properties for the F404 engine are listed in Table 1, based on Reference 10. For the single engine, max A/B case the effect of a second engine operating at idle power was ignored.

The results are shown in Table 2, in terms of $\mu$, the augmentation ratio and $T_2$, the fully mixed gas temperature in the augmentor duct which was taken as a measure of the thermal loading on the duct. Notable features of Table 2 are:

- The sensitivity of augmentor performance to the levels of the two loss coefficients, which varied from zero to values which represent somewhat higher pressure drops than might be expected in practice.

- The similar levels of augmentation ratio for IRP and max A/B operation of a single engine. This is consistent with behaviour observed in a test cell for F-14 aircraft with TF30 engines, where pumping of cooling flow remained constant during excursions into afterburning thrust[11].

- Levels of mixed flow temperature for single engine, max A/B operation which are substantially higher than those for two engines at IRP, due not only to the higher total fuel flow, but also to the fact that the quantity of cooling air entrained by the single jet is only about three quarters of that entrained by the two jets at IRP, regardless of aerodynamic losses. Single engine, max A/B operation is thus confirmed as the critical condition for thermal design of the augmentor ducts, whilst twin engine, IRP operation is the limiting condition from the point of view of handling the cooling air flow in the installed engine testing facility.

- Mixed flow temperatures which are quite modest overall, even with the largest levels of loss coefficient. Notwithstanding that some duct components may experience temperatures higher than that calculated for fully mixed flow, this tends to confirm the conservatism of the early choice of augmentor duct dimensions.

2.2.3 Assessment of duct size

Theoretical curves of augmentation ratio $\mu$ are plotted against augmentor duct area ratio $\nu$ for single engine, max A/B operation and for twin engine, IRP operation in Figures 6 and 7 respectively. Curves are shown for the four different combinations of the two loss coefficients used for constructing Table 2. Figure 6 includes a vertical scale of fully mixed exhaust gas temperature, which is directly related to the augmentation ratio. Superimposed on the theoretical curves in Figures 6 and 7 are data based on correlations of scale model test results relating to operational facilities, reported in References 7 and 11. A point representing the design performance of an installation used for testing F404 engines in CF-18 aircraft[12] is also included in each Figure. Notwithstanding the wide possible variation in augmentor designs, and the corresponding possible variation in effective loss characteristics, the trends exhibited by these empirical data, all of which are reported to have been validated to some degree by full scale measurement, bear a reasonably consistent relationship to the theoretical curves.

The designer of the RAAF Williamtown facilities nominated a maximum temperature of 525-550 $^{o}$C for the acoustic lining materials[3,4], and a target figure for augmentation ratio with single engine, max A/B operation of 7-8 to allow for the likelihood that some duct components may be subjected to gas temperatures in excess of the fully mixed flow temperature[13]. Figure 6 indicates that, for any reasonable level of aerodynamic losses, the 4.8m x 4.8m duct cross sections featured in the early augmentor designs could be expected to exceed these requirements by a large margin. This, of course, assumes that the flow in the augmentor ducts will be well behaved, with no tendency towards impingement of the uncooled jets on the duct walls. The use of square (as distinct from, say, circular) duct cross sections probably also calls for conservative interpretation of Figure 6.

2.3 Revised Designs

2.3.1 Augmentor configurations

In the light of the above considerations, and under pressure to reduce construction costs, the designs were revised incorporating a number of changes. The new designs are shown in outline, together with leading dimensions, in Figures 8 and 9. The main changes were as follows:

- The augmentor duct cross sections were reduced to 4.2m x 3.5m and 3.5m x 3.5m for the installed and uninstalled engine facilities respectively, the greater width in the installed engine augmentor being specified because of the lateral separation of the two engines in the aircraft.

- The inlet arrangements were redesigned to limit the airflow velocities in the immediate vicinity of the test aircraft, and to effectively eliminate the depression in the uninstalled engine test enclosure. Primary augmentor tubes were added, of obround cross section in the case of the installed engine facility and round for the uninstalled engine facility. These primary tubes, which are identified in Figures 8 and 9, were designed to entrain part of the cooling air, while most of the air entered via the larger secondary inlets. In the case of the uninstalled engine facility the secondary inlets were equipped with acoustic splitters, but the splitters in the overhead inlet to the engine test bay were eliminated.

- The exhaust stacks, splitters and turning vanes were replaced by deflector ramps designed to minimise exhaust blast effects at ground level. To compensate for the loss of acoustic attenuation due to elimination of the exhaust stacks, the proportional lengths of the acoustically lined augmentor ducts were increased by about two duct heights.

### 2.3.2 Pumping performance

The addition of primary augmentor tubes could significantly alter the overall entrainment characteristics, since the augmentors effectively became two-stage ejectors. However, as will be seen, the primary tubes were subsequently reduced to vestigial proportions on the basis of model test results, such that the above performance calculations could be expected to remain valid, with no need to resort to the more complex two-stage ejector theory[9].

Figure 6 indicates that the required pumping performance should still be comfortably exceeded with the reduced augmentor duct dimensions, especially since the exit loss coefficients could be expected to be reduced by elimination of the exhaust stacks. This is consistent with the observation that the augmentor area ratios remained substantially higher than the corresponding ratios for comparable existing facilities used by the US Navy at NAS Miramar[11], the Canadian Defence Forces at CFB Baden[12] and the Republic of Singapore Air Force at Paya Lebar[14], for example.

### 2.3.3 Jet symmetry considerations

Provided the mixing flow in the augmentor ducts is well behaved, the extent to which the wall linings may be subjected to excessive thermal or aerodynamic loading is largely a function of possible jet asymmetry or misalignment. Reference 7 offers an empirically based procedure for assessing these effects. Application of the procedure to the configurations of Figures 8 and 9 indicated that, for any plausible level of misalignment, the wall temperatures would remain below the 525$^{o}$C limit nominated by the designer.

In the case of installed engines in the F/A-18, these concerns are further alleviated by the fact that the axes of the two engine exhaust nozzles, whilst spaced apart laterally, are canted inwards at a total included angle of about $4^{o}$. As Figure 10 shows, with correct aircraft alignment, this has the favourable effect that the downstream projections of the jet axes in the installed engine facility cross on the augmentor duct centreline at a point about mid-way along the length of the duct.

## 3. MODEL TESTS

### 3.1 Purpose of Tests

Whilst the augmentor designs were regarded as conservative in terms of duct size, they also had some unusual features which introduced an element of unpredictability to the prospective flow behaviour. These features included the secondary air inlet arrangements, which were not three-dimensionally symmetrical, the rectilinear duct cross sections and, to a lesser degree, the exhaust deflector ramps. Aerodynamic testing of scale models of the two facilities was undertaken, with the following purposes:

- To confirm that the augmentor internal flow was not likely to behave in such a way as to cause excessive local thermal or aerodynamic loading.
- To confirm the predicted levels of pumping performance.
- To optimise detailed aspects of the aerodynamic designs.
- To assess the tolerance of the internal flow to inlet asymmetry and jet misalignment.

### 3.2 Model Construction

Models representing the two facilities were built to 1/45 scale, reproducing the internal geometries of the exhaust augmentors as they were defined following the design revision outlined in Section 2.3 above. The models were constructed mainly from timber and glass, with no attempt to simulate detailed internal surface features such as perforated acoustic linings.

Photographs of the two models appear in Figure 11. In the vicinity of the air inlets, only those features thought to be directly relevant to the augmentor duct internal flow were represented; as can be seen, most of the test bay structures were omitted. The model of the installed engine facility is shown in partly modified form, with bellmouth fairings added to the secondary air inlets, whilst the other model appears in original, unmodified form.

The engine exhaust jet was simulated with unheated, pressurised air issuing from a convergent-divergent nozzle of correct geometrical scale. All tests were arranged to represent single engine, max A/B operation, since this was the critical case governing the thermal design, and also the condition thought more likely to lead to problems with flow asymmetry in the installed engine augmentor.

### 3.3 Flow Scaling

Given that strict simulation of the augmentor flow was not possible with an unheated jet, the level of simulation which could be achieved, and the best means of achieving it, had to be considered.

The entrainment properties of a jet, in a one-dimensional sense, are generally regarded as being a function of jet momentum[7]. If this were wholly the case, then a compressible jet with a given pressure ratio and fixed gas properties, issuing from a nozzle of fixed dimensions into an ideal loss-free ejector, would entrain flow at a rate which is independent of its temperature, because jet momentum

$$I = PA\gamma M^2$$

is independent of temperature. This is not sustained by ejector theory. Figure 12, which contains curves calculated for a one-dimensional ejector geometry equivalent to the uninstalled engine augmentor in Figure 9, shows that an increase in jet temperature ratio from 1 to 7 (equivalent to transition from isothermal conditions to max A/B jet temperature), with constant gas properties, theoretically results in a reduction in entrained air flow at loss-free conditions which corresponds to a reduction in entrained flow inlet Mach number of some 11 per cent. When the appropriate variation of gas properties resulting from the combustion process is superimposed on the temperature increase, the reduction in entrained flow inlet Mach number becomes about 27 per cent.

It would be possible to adjust the size, pressure and/or Mach number of the unheated model jet to reproduce precisely the momentum of the hot gas jet or, going a step further, to yield a level of entrained flow inlet Mach number which (theoretically) corresponds with the full scale situation. However, this did not seem justified when complete simulation would remain unattainable with the isothermal flow. The simpler approach, adhering to geometric similarity with the correct jet pressure ratio, was adopted. To simulate max A/B operation, this required a nozzle blowing pressure of 340 kPa. The augmentation ratios measured in the isothermal models could be translated to the full scale, hot jet situation with reasonable confidence, as will be seen below.

Only loose simulation of the three-dimensional mixing flows in the full scale augmentor ducts was possible with the cold air jet. Lower rates of mixing could be expected because of the reduced density differentials[15], and the gas velocities were different. Nevertheless, the measured pressure and mean velocity distributions could be expected to be qualitatively similar to the full scale distributions, notably in respect of any asymmetrical flow behaviour.

### 3.4 Nozzle Alignment

The two engines in the F/A-18 aircraft are installed with their exhaust nozzle centrelines laterally spaced 0.9m apart and, as noted earlier, canted inwards with an included angle of about $4^{o}$. In the normal arrangement representing single engine operation in the installed engine model, the single nozzle was therefore displaced

laterally 0.45m (full scale)[#] from the duct centreline and angled $2^{o}$ towards the centreline. The exit plane of the nozzle was normally positioned 1.4m upstream of the commencement of the throat of the primary augmentor tube, and in the vertical plane the nozzle axis was placed on and parallel to the duct centreline. This arrangement is shown in plan view in Figure 13. For investigative purposes some tests were conducted with different arrangements from that shown.

In the uninstalled engine model, the nozzle axis was positioned on and parallel to the duct centreline, with the same lengthwise spacing as that shown in Figure 13.

### 3.5 Measurements and Observations

Surveys of mean air velocity in the augmentor ducts were made using a pitot-static probe aligned parallel with the duct axis, driven by the traverse mechanism shown mounted above the model ducts in Figure 11. The measurements could be made both at the "exit" flow stations as defined in Figures 8 and 9 and at intermediate stations approximately 2 duct heights further upstream. The pressures were measured with strain gauge transducers and recorded using an X-Y plotter. The duct mass flows were determined by integrating the velocities measured at the exit planes, and knowledge of the jet mass flow delivered through the choked primary nozzle permitted the augmentation ratios to be calculated.

Static pressure distributions along the inside of the upper surfaces of the ducts were measured with flush tappings. Flow visualisation was carried out with both schlieren apparatus and wool tufts.

### 3.6 Effect of Duct Exit Geometry

#### 3.6.1 Presence of deflector ramp

The model of the uninstalled engine facility was used for initial investigation of the influence of the exhaust deflector ramp. Figure 14(a) shows the distribution of velocity at the augmentor duct exit and the intermediate flow station, as initially measured with the ramp in position. It appeared likely from comparison of these maps that the distortion in the vertical plane evident in the exit plane distribution was associated with the proximity of the ramp to the exit flow station. This was confirmed by an experiment in which the ramp was removed; the resultant velocity distribution at the duct exit, shown in Figure 14(b), displays very little evidence of distortion in the vertical plane. The consistent bias of the peak velocity towards one side of the duct seen in Figure 14 was subsequently found to be associated with the primary augmentor tube which, for these early tests, was relatively long. This effect is discussed further in Section 3.7 below.

Clearly, the deflector ramp had a substantial upstream influence on the duct flow behaviour. In addition to the change in exit flow distribution seen in Figures 14(a) and 14(b), the isothermal augmentation ratio increased from 4.58 to 5.28 when the ramp was removed. There was obviously a significant back-pressure effect due to the ramp; direct evidence of this appears in Figure 15, which compares the two

---

[#] All dimensions quoted relate to full scale facilities

static pressure distributions along the upper surface of the duct corresponding with Figures 14(a) and 14(b).

Figure 15 indicates that the static pressure at the exit flow station, as defined here, was well below atmospheric pressure when no ramp was present, and still marginally sub-atmospheric with the ramp in place. Although the static pressure on the upper surface was not necessarily fully representative of the mean static pressure at a given flow station, this suggests that the assembly downstream of the defined exit plane, including the divergent side-walls and the inner chamfer on the duct roof, functioned as a diffuser with measurable pressure recovery. In terms of the upper surface static pressure, this effect approximately compensated for the pressure rise imposed by the ramp.

3.6.2 Ramp position

To relieve the adverse influence of the ramp, whilst preserving its primary function, it was displaced by half a duct height (1.75m full scale) downstream from the duct exit plane. In the test models it was expedient to effect this change by shortening the duct roof, as shown in Figure 16; it was anticipated that any adverse effect of the reduction in enclosed duct length would be minimal.

The effects on the exit velocity distribution, augmentation ratio and streamwise static pressure distribution in the uninstalled engine model are shown in Figures 17 and 18, in this case with a shortened primary augmentor tube. The vertical plane flow distortion was reduced, and the entrained cooling flow was increased by 11 per cent due to the reduced back-pressure which is evident in Figure 18.

Similar benefits were measured in the installed engine model, using a coaxially placed jet to isolate the effects. Figure 19 shows the exit velocity distributions, in this case translating to an increase in isothermal augmentation ratio of 12 per cent resulting from the change in exit geometry. Static pressure distributions were not available.

3.7 Effect of Primary Augmentor Tube Geometry

3.7.1 Installed engine facility

In early tests with the asymmetrically disposed jet, unexpected distortion was observed in the augmentor duct flow which was subsequently found to result from the influence of the primary augmentor tube. The effects are illustrated in Figure 20 which shows, for the originally proposed primary tube geometry, how the velocity distributions at both the intermediate and exit flow stations varied as the jet nozzle alignment was changed from coaxial, through simple lateral displacement, to the "normal" combination of lateral and angular displacement defined in Figure 13. Each velocity map includes an indication of the local position of the projection of the nozzle axis; as can be seen, lateral displacement of the hot jet had an exaggerated effect on the distortion of the downstream flow, relative to that which may have been expected on the basis of simple projection of the jet axis. The local peak velocity (and, by implication, the local peak temperature in the case of a hot jet) was increased, as was the risk of hot gas impingement on the duct lining.

By a process of elimination, the origin of these effects was traced to interaction between the jet and the primary augmentor tube. When the jet was displaced laterally from a coaxial position, it tended to become attached to the nearer wall of the primary tube by a mechanism akin to the Coanda effect, and was thus diverted further in the direction of the original lateral displacement, negating the otherwise beneficial effect of the $2^{o}$ cant of the nozzle axis back towards the duct centreline. In addition to the adverse effect of the resulting asymmetrical flow in the main augmentor duct, in a full scale facility this would cause significant (probably unsteady) lateral force on the primary tube structure, as well as heat exposure of the tube wall. The nature of the phenomenon is revealed in the schlieren photograph in Figure 21, showing the asymmetrically disposed jet being deflected in its passage through an obround tube in isolation.

The effect of primary tube geometry on the magnitude of this effect was investigated in the installed engine facility model by varying the length, overall scale and aspect ratio of the tube. Figure 22 shows velocity profiles measured on the mid-height horizontal plane at the exit of the main augmentor duct, with "normal" (asymmetrical) jet alignment, and with four different lengths of primary tube of 1.5m x 2.4m obround cross section . For all but the very shortest tube, the lateral location of the peak velocity at the main duct exit was displaced a significant distance from the projection of the nozzle centreline. Full exit velocity distributions, and corresponding values of augmentation ratio, are shown for three of the primary tube lengths in Figure 23; reducing the tube length had a small adverse effect on the augmentation ratio.

The effect of increasing the cross-sectional width of the 3.1m long tube is shown in Figure 24. Some benefit is apparent, but the effect of interaction between the jet and primary tube remained substantial.

Lateral velocity profiles are shown in Figure 25 for two relatively short primary tubes which were approximately geometrically similar but of different size. The degree of jet deflection increased when the tube cross-sectional size was reduced so as to bring the jet into closer proximity with the tube wall, despite the simultaneous reduction in tube length.

The primary tube dimensions adopted for the installed engine augmentor on the basis of the above observations were as shown in Figure 26(a). With this configuration the jet/tube interaction was arguably favourable since, on the evidence of Figure 22, the 1.3m long tube deflected the jet core from the projection of the nozzle axis by a small degree so that it became approximately centralised at the main duct exit. The effect on augmentation ratio of reducing the tube length was insignificant. Adoption of this geometry for the full scale facility involved an implied assumption that the effects described above were quantitatively independent of jet temperature; an uncertain although probably not dangerous assumption.

### 3.7.2 Uninstalled engine facility

As observed above, the primary tube geometry became important in the context of main duct flow symmetry when the jet nozzle was displaced from a coaxial position. Since the uninstalled engine, mounted on its test stand, should always be

aligned coaxially with the augmentor, this should not be a major issue with the uninstalled engine facility. However, the duct flow symmetry was found to be sensitive to quite small lateral displacements of the jet in the relatively long, narrow (2.3m x 1.3m dia) primary tube originally prescribed for this facility. This is evidenced in Figure 14, which reveals lateral distortion of the main duct velocity distributions, albeit small, due to interaction of the primary tube with a nominally coaxial jet which was actually slightly misaligned. Consequently, it was recommended that the tube be shortened to 1.2m, a length proportionally equal to that adopted for the installed engine facility.

The recommended geometry is shown in Figure 26(b). The smaller (1.3m) diameter, relative to the 1.5m vertical dimension adopted for primary tube in the other facility, was preferred so as to reduce the entrained air flow through the primary tube and minimise the air velocity over the engine test stand, and was regarded as tolerable in this basically coaxial facility.

As with the installed engine facility, the effect on augmentation ratio of reducing the tube length was minimal. This is evident from Figure 27, where augmentation ratio is plotted against the length of the 1.3m diameter tube. The points on the full curve were measured before the main duct exit configuration was changed, but only one experimental point was available for the modified geometry.

### 3.8 Effect of Inlet Fairings

#### 3.8.1 Installed engine facility

On the basic model it was observed by the use of wool tufts that gross flow separations occurred at the upstream edges of the secondary inlets, and also at the vertical corners where the secondary inlet ducts were integrated with the main augmentor duct. These flow features, shown diagrammatically in Figure 28(a), added to the aerodynamic losses, reduced the cooling flow and threatened to impair the symmetry of the flow in the main duct. As part of the optimisation exercise, these deficiencies were treated by adding bellmouth profiles to the edges of the secondary inlets and fairing the vertical duct corners, as indicated in Figures 28(b) and 28(c).

Figure 29 shows the effect of these modifications on the flow adjacent to the surface of the main duct side-walls immediately downstream of the inlet corners, as revealed by tufts attached to one of the walls. The diagram at the top of the Figure indicates the extent of the tufted area, and the means of visual access through the opposite glass wall. Both the profiled inlets and the faired corners contributed to control of the separated flow in the tufted area.

The corresponding effects on the velocity distributions at the main duct exit are shown in Figure 30. The modifications resulted in a 7 per cent increase in isothermal augmentation ratio, the additional flow being concentrated towards the centre of the exit cross section, which is perhaps surprising. It is suggested that the flow separations in the inlet region, being three-dimensional in nature - note, for example, the evidence of vortical flow in the surface flow pattern in Figure 29(b) - had shed vortices into the duct flow which were manifested in increased losses towards the core of the flow.

The velocity distribution appearing in Figure 30(c) was representative of the configuration for the installed engine facility which was regarded as optimum. The corresponding isothermal augmentation ratio was 5.99.

3.8.2 Uninstalled engine facility

A similar process of inlet geometry refinement was undertaken with the uninstalled engine facility model. In this case the presence of the secondary inlet splitters made the flow less prone to separation from the vertical inlet lips, but profiling of the upper horizontal lip was obviously beneficial. Fairings were also added to the inner duct vertical corners, as with the installed engine facility.

Pronounced vortices were observed to be shed from the sharp edges representing the external overhangs of the engine test bay roof, located immediately outside and above the secondary air inlets. One of these edges is evident in Figure 11(b). The effect of the vortices as they were ingested by the augmentor was unknown, but thought unlikely to be beneficial. An indication of the location of one of the vortices, and the modification introduced to improve the flow behaviour, are indicated in Figure 31.

The sum effect of these modifications on the exit velocity distributions is shown in Figure 32. In this case there was a much smaller increase in the augmentation ratio - about 2 per cent - probably because the presence of the inlet splitters limited the benefit to be gained by reducing the inlet lip separation losses. Figure 32(b), with an isothermal augmentation ratio of 4.97, is regarded as representing the performance of the optimum configuration for the uninstalled engine augmentor.

3.9 Sensitivity to Inlet Asymmetry

3.9.1 Inlet blockage

Because the two secondary flow inlets in the uninstalled engine facility were open to the elements, the possibility of partial blockage of one of the inlets, by blown debris for example, could not be overlooked. In the process of investigating the causes of augmentor flow lateral distortion, tests were carried out with asymmetrical blockage of the secondary flow inlets which could be regarded as representative of this condition. One of the three passages between the acoustic splitters was blocked, on each side in turn, as indicated in Figure 33. The augmentor geometry was an early one which included none of the refinements discussed above, but the results were qualitatively valid.

The graph in Figure 33 shows mid-height exit velocity profiles for the two asymmetrical conditions compared with the profile measured with the normal symmetrical arrangement. The resulting levels of distortion, while far from desirable, demonstrated reasonable tolerance to inlet asymmetry in view of the extreme nature of the blockages involved.

### 3.9.2 Cross-wind

The uninstalled engine facility was arguably also vulnerable to the effect of cross-winds on the secondary inlet flow. This was tested on the model using an electric fan, with the results shown in Figure 34. With wind velocities up to 20 m/s normal to the augmentor centreline, directed at one of the secondary inlets, the effect on the symmetry of the duct flow was measurable, but small. This was not surprising, in view of the fact that even the highest wind velocity was small relative to the local velocity of the entrained air at the secondary inlets. Whilst the evidence was again qualitative, it indicated that the adverse effect of cross-wind could be discounted.

## 3.10 Sensitivity to Jet Misalignment

Tests were carried out to determine the sensitivity of the augmentor flow to jet misalignment in the vertical plane. Here the main focus of concern was the installed engine facility because, although means were to be provided for adjustment and restraint of the test aircraft attitude, some variation of undercarriage geometry might be expected both between different aircraft and, with a given aircraft, during engine thrust excursions. The tests were conducted with the fully refined model configuration.

Figure 35 compares velocity profiles measured on the vertical centreline at the duct exit plane, with:

- "normal" jet alignment
- the jet parallel to the augmentor centreline but displaced downwards by 100 mm (full scale)
- the nozzle displaced downwards by 100 mm, and also tilted downwards by an angle (approximately $1^{o}$) which would apply had the 100 mm displacement been caused by rotation of the aircraft about its main undercarriage.

These displacements were more than double the maximum movement measured on a restrained aircraft during a trial engine run with extreme power excursions[16].

For each case, Figure 35 includes an indication of the height of the linear projection of the jet nozzle axis where it intersected the duct exit plane. As can be seen, each jet displacement produced an effect on the exit velocity profile which was slightly exaggerated, relative to the effect which might have been qualitatively estimated on the basis of the shift in the local position of the nozzle axis projection. Consistent with observations discussed in Section 3.7 above, this almost certainly resulted from interaction between the jet and the primary augmentor tube.

Observations of the effects of other, less systematic, variations of jet alignment in the models of both the installed and uninstalled engine facilities, once the primary augmentor tubes had been modified to their shortened configurations, were consistent with the above. Within reasonable limits of misalignment in either the vertical or horizontal planes, the path of the jet core in the augmentor tube did not depart far from the linear projection of the nozzle axis.

## 4. ESTIMATE OF FULL SCALE PUMPING PERFORMANCE

The cooling flow augmentation ratios measured with unheated air jets in the fully optimised models of the installed and uninstalled engine facilities, were 5.99 and 4.97 respectively. These figures could be translated to the full scale, hot jet situation with the aid of the theory described earlier. As in Section 2.2 above, the procedure assumed that the effects of incomplete kinetic and thermal mixing in these relatively long ducts were of second order importance. Any such effect should act in a conservative sense - increasing the augmentation ratios in the full scale facilities relative to the predicted values - because of the higher rates of mixing which may be expected with hotter jets. As noted earlier, the effects on pumping performance of the small primary augmentor tubes featured in the ultimate designs could safely be ignored.

It was arguably possible to use the static pressures measured in the models to arrive at values for the two loss coefficients, $k_1$ and $k_2$, which could in turn be used to calculate the corresponding full scale augmentor performance. It will be recalled, however, that for theoretical convenience the overall losses for the system were notionally lumped into these two coefficients; whilst they performed a useful theoretical function, in reality the two coefficients could not therefore be represented by measurable pressure differences. The approach used instead, for the purpose of arriving at loss characteristics which matched the measured pumping performance, was to adopt two possible extremes for apportioning the losses between $k_1$ and $k_2$: $k_1 = 0$ with $k_2$ taking the value necessary to account for the measured performance, and vice-versa.

In Figure 36, the theoretical value of augmentation ratio in the installed engine facility is plotted against loss coefficient, in two bands: the lower one represents isothermal flow, while the other applies with jet conditions appropriate to the F404 engine in maximum afterburner, including differential gas properties as well as temperature. The upper and lower boundaries of each band correspond to the two extreme combinations of $k_1$ and $k_2$ defined above. The experimental value of 5.99 for the isothermal augmentation ratio in the model of the installed engine facility, related to the boundaries of the lower band, defines the limits of the plausible ranges of $k_1$ and $k_2$ in the model; when applied in turn to the upper band, these limits indicate that the augmentation ratio for the full scale facility should be in the range 12.5-13.5.

Using data from experiments with varying jet temperature, Reference 7 offers a different procedure for correcting pumping performance for the effects of temperature. On the basis of the above isothermal model result, this suggests a value of 14.1 for augmentation ratio in the full scale installed engine facility.

The theoretical estimation of the pumping performance of the full scale uninstalled engine augmentor, using the same procedure as that applied in Figure 36, is set out in Figure 37. The measured isothermal model augmentation ratio of 4.97 translated to a full scale value in the range 10.2-11.3. The empirical procedure in Reference 7 yielded a figure of 11.5.

The graph of augmentation ratio against duct cross-sectional area for single engine, max A/B operation, previously shown in Figure 6, is reproduced in Figure 38 with added symbols which represent the above four estimates of full scale augmentor performance. The values for the installed engine facility are somewhat higher than the earlier predictions based on empirical experience with other configurations; however, it should be recalled that they were determined from the highest level of performance recorded during the present model tests, and the models did not have internal surface roughness representative of acoustic linings. It has been observed that this latter effect can account for a 10 per cent difference in pumping performance[7]. The fact that the figures based on the model tests for the uninstalled engine facility look lower against the framework of Figure 38 may be ascribed to the higher aerodynamic loss associated with the acoustic splitters in the secondary inlets of that configuration.

## 5. FINAL DESIGNS

The designs for the two facilities, as ultimately constructed, are shown in outline in Figures 39 and 40. They incorporated the essential features of all of the refinements described in the foregoing sections, and their aerodynamic performance may be expected to be consistent with the above predictions.

## 6. CONCLUSION

Aerothermodynamic aspects of the design of exhaust augmentors for upgraded F/A-18 engine run-up facilities at RAAF Williamtown have been appraised in some detail. In the initial development of the designs, changes were recommended to improve the aerodynamic characteristics of the exhaust augmentors and eliminate high risk features. A quantitative assessment was made of the cooling flow pumping performance of the two augmentors, which led to a significant reduction in size of the augmentor ducts. The revised designs were still regarded as conservative, with cooling flow rates predicted to exceed the design requirements by comfortable margins.

Aerodynamic model tests were undertaken, using unheated air jets to represent the engine exhausts. It was confirmed that the basic designs were sound, provided that certain requirements were met. Foremost amongst these were the dimensions of the primary augmentor tubes; these had to be chosen to avoid adverse aerodynamic interactions with the engine jets, which caused distortion of the augmentor duct flow and risked overheating of the duct linings. Other features addressed included the duct exit geometry and the detailed design of the secondary flow inlets. As well as providing data for optimising the designs, the model tests confirmed the pumping performance of the refined augmentor designs and demonstrated their tolerance to both inlet asymmetries and reasonable levels of jet misalignment.

ARL's contribution to the design process for the upgraded facilities was confined to aerothermodynamic behaviour, and did not address acoustic, structural or materials aspects of the designs. The benefits from this exercise, either established or in prospect, include significant reduction of the technical risks, reduced construction costs, increased operational effectiveness and longer service life.

**ACKNOWLEDGEMENT**

The contribution of Mr Martin Fisher to design, manufacture and operation of the model test rigs is gratefully acknowledged.

## REFERENCES


1. S.A. Fisher and A.M. Abdel-Fattah, "Aerodynamic Model Tests of Exhaust Augmentors for F/A-18 Engine Run-Up Facility at RAAF Williamtown - Summary Report". ARL, Aero Propulsion Tech Memo 458, December 1988.

2. S.A. Fisher and A.M. Abdel-Fattah, "Aerothermodynamics of Exhaust Augmentors for Ground Running of F/A-18 Engines". Australian Aeronautical Conference, Melbourne, October 1989.

3. L.A. Challis and Associates Pty Ltd, "Williamtown NTF Run-up Facility - Description of Proposed Reconstructed Facility". Report No. 4990E-2-86, August 1986.

4. L.A. Challis and Associates Pty Ltd, "Tentative Design Brief - Williamtown NTF Run-up Facility for Department of Administrative Services, Construction Services". Report No. 4990G-2-88, June 1988.

5. S.A. Fisher and R.D. Irvine, "Air Augmentation of Rockets for Low Speed Application". Fifth International Symposium on Air Breathing Engines, Bangalore, February 1981.

6. F.M. Oran and M.I. Schiff, "Design of Air-Cooled Jet Engine Testing Facilities". ASME, 1979 Israel Joint Gas Turbine Congress, Haifa, July 1979.

7. J.L. Grunnet, "An Aerodynamic and Acoustic Test of a 1/15 Scale Model Dry Cooled Jet Aircraft Run-Up Noise Suppression System". Fluidyne Corporation, 1975.

8. B. Quinn, "Ejector Performance at High Temperatures and Pressures". J. Aircraft, Vol 1 No 12, December 1976.

9. A.M. Abdel-Fattah, "A Theoretical Study of Two-Stage Thrust Augmenting Ejectors". ARL, Report Aero Prop 166, November 1984.

10. General Electric Co., F404 Status 10 Engine Performance Specification, March 1984.

11. J.L. Grunnet and E. Ference, "Model Test and Full-Scale Checkout of Dry-Cooled Jet Runup Sound Suppressors". J. Aircraft, Vol 20 No 11, October 1983.

12. Canadian Defence Staff, Private communications, 1987-88.

13. L.A. Challis and Associates Pty Ltd, Private communication, May 1989.

14. "The Hush that Fell over Paya Lebar". Southeast Asia Building News, March 1988.

15. G.L. Brown and A. Roshko, "On Density Effects and Large Structure in Turbulent Mixing Layers". J. Fluid Mechanics, Vol 64 Part 4, 1974.

16. RAAF, Private communication, 1988.

**TABLE 1 F404 ENGINE DATA**

| | IRP | MAX A/B |
|---|---|---|
| Exhaust Total Temperature (K) | 945 | 2018 |
| Exhaust Total Pressure (Atm) | 3.942 | 3.311 |
| Nozzle Exit Static Pressure (Atm) | 0.792 | 0.554 |
| Nozzle Exit Mach Number | 1.642 | 1.853 |
| Nozzle Area ($m^2$) | | |
| - Throat | 0.151 | 0.243 |
| - Exit | 0.185 | 0.371 |
| Exhaust Gas $\gamma$ | 1.328 | 1.257 |
| Exhaust Gas $C_p$ (kJ/kgK) | 1.163 | 1.405 |
| Total Fuel Flow (kg/s) | 1.109 | 4.007 |
| Exhaust Mass Flow (kg/s) | 65.70 | 68.34 |

**TABLE 2 THEORETICAL PUMPING PERFORMANCE**

Augmentor Cross Section 4.8 X 4.8 $m^2$

| $k_1$ | $k_2$ | $\mu$ | | | $T_2$ °C | | |
|---|---|---|---|---|---|---|---|
| | | 1Eng IRP | 2Eng IRP | 1Eng MAX AB | 1Eng IRP | 2Eng IRP | 1Eng MAX AB |
| 0 | 0 | 24.4 | 16.2 | 24.8 | 45 | 57 | 107 |
| 1 | 0 | 17.8 | 12.0 | 18.8 | 56 | 72 | 135 |
| 0 | 2.5 | 12.5 | 8.2 | 12.4 | 71 | 95 | 191 |
| 1 | 2.5 | 11.2 | 7.4 | 11.3 | 77 | 103 | 205 |

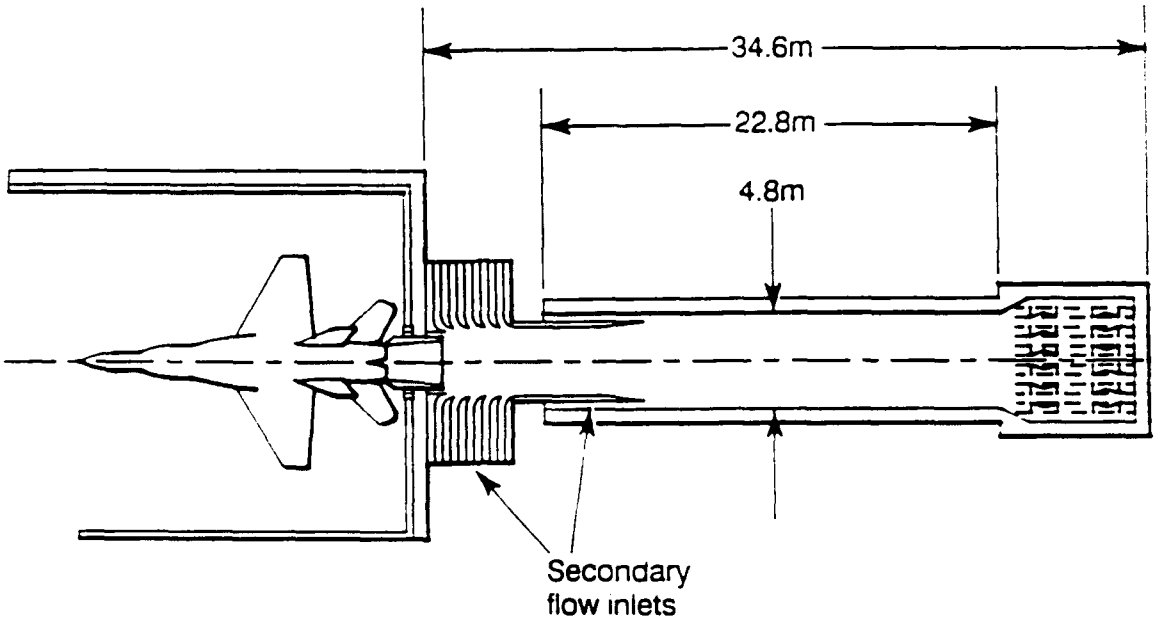


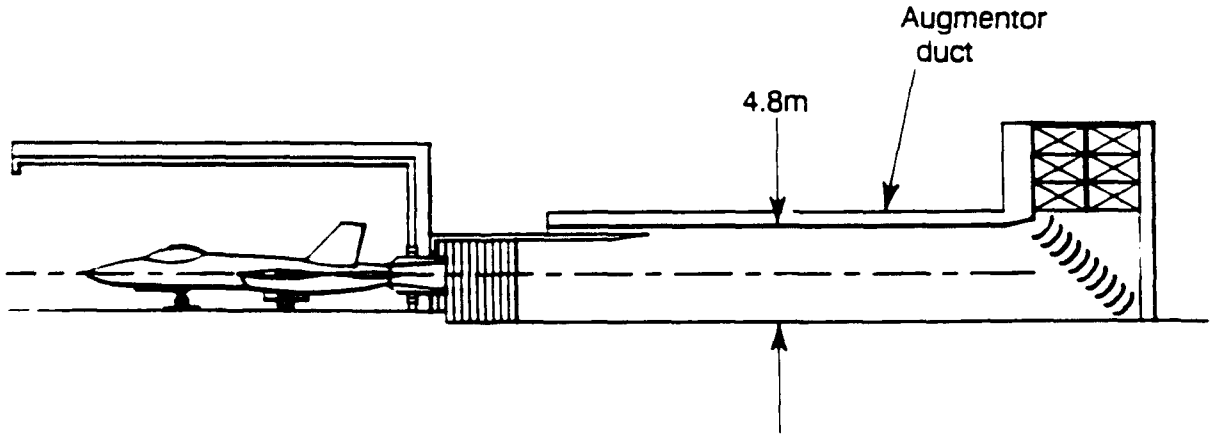


FIGURE 1. INSTALLED ENGINE TEST FACILITY - EARLY PROPOSAL

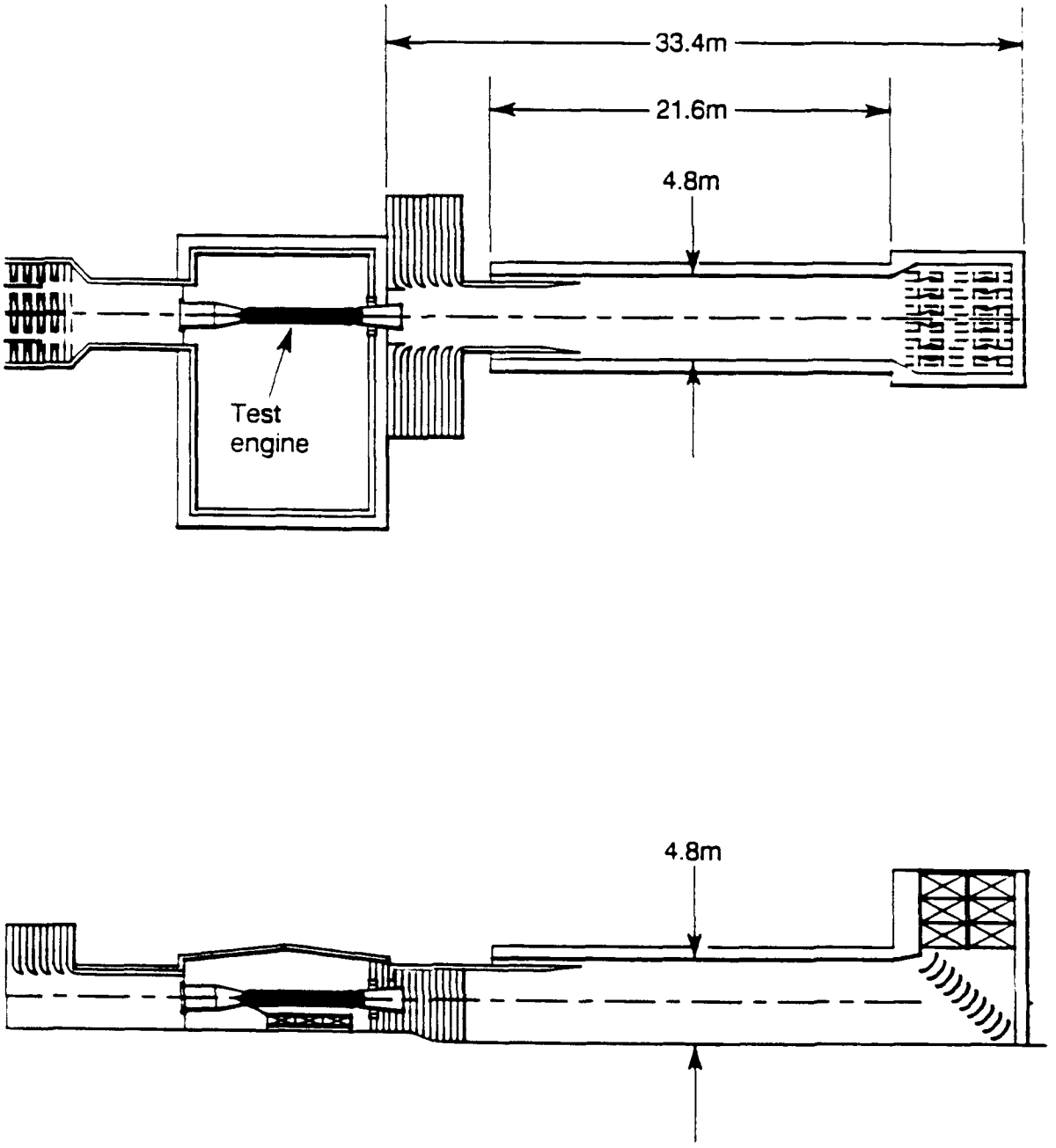


FIGURE 2. UNINSTALLED ENGINE TEST FACILITY - EARLY PROPOSAL

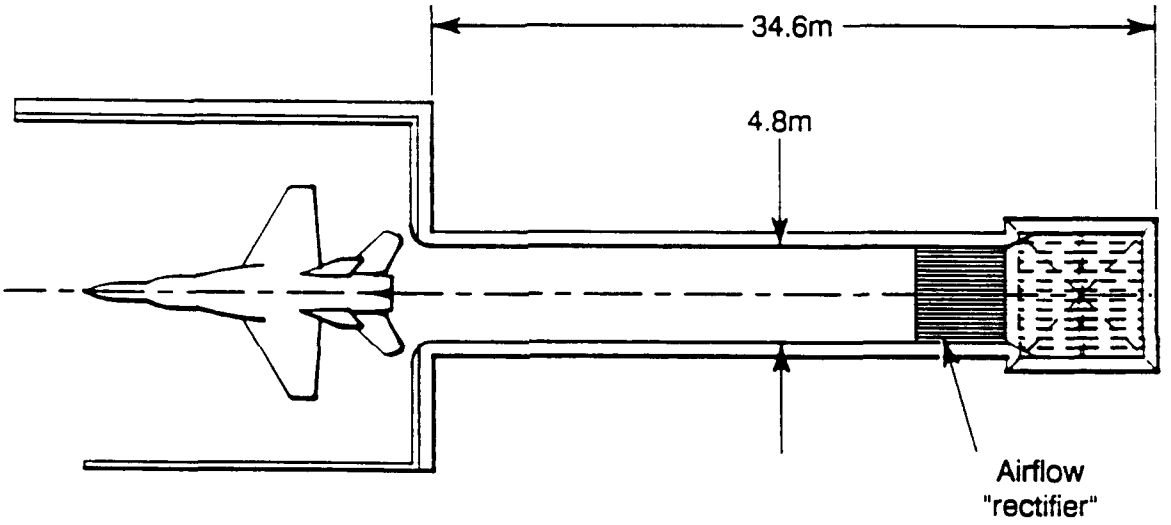


FIGURE 3. INSTALLED ENGINE TEST FACILITY - SIMPLIFIED INLET

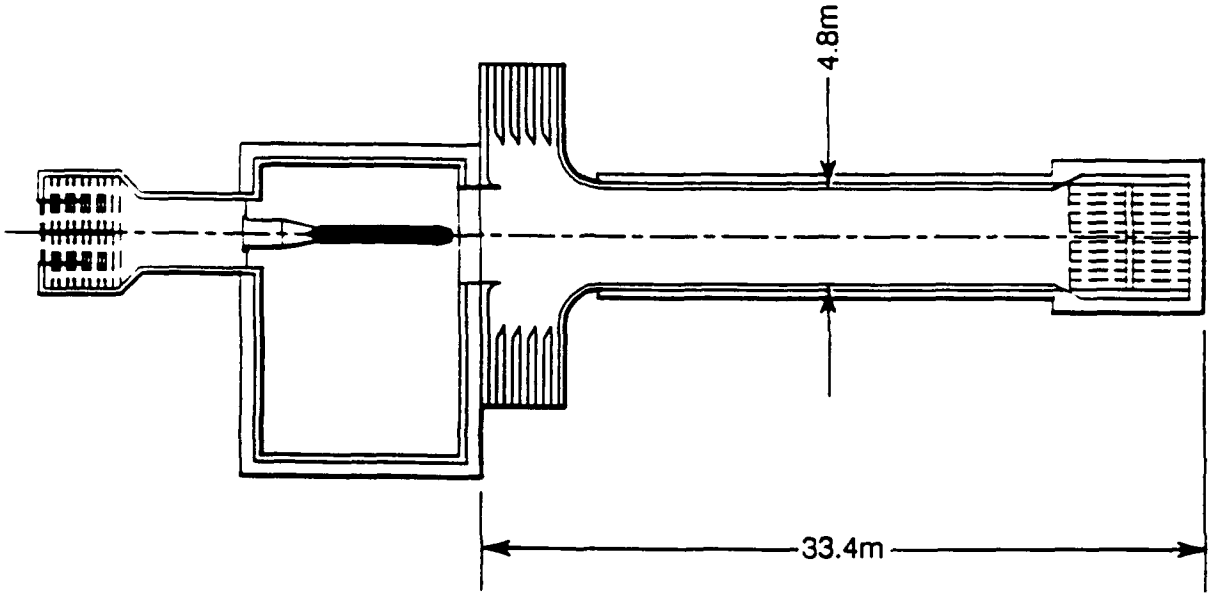


FIGURE 4. UNINSTALLED ENGINE TEST FACILITY - SIMPLIFIED INLET

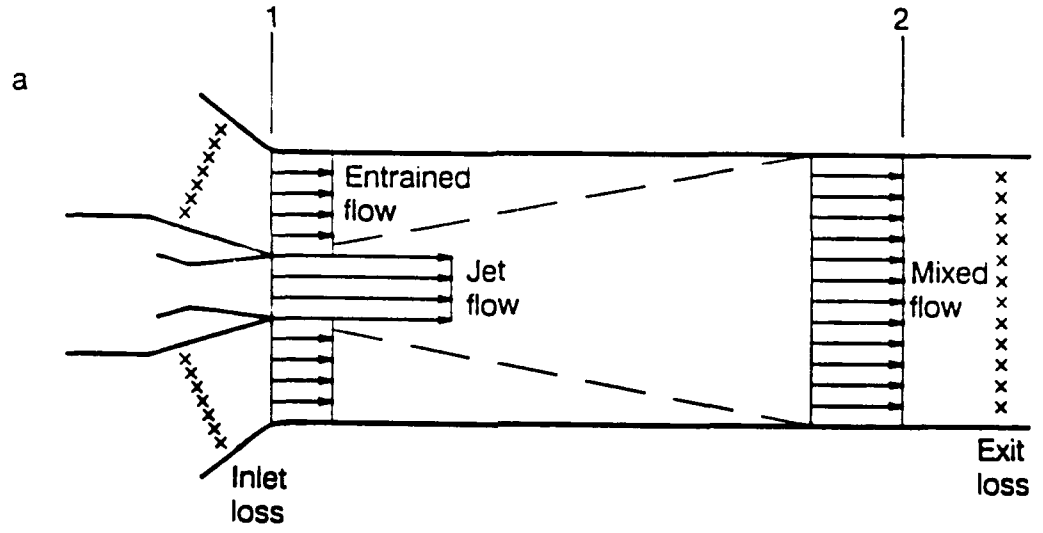


FIGURE 5. THEORETICAL EJECTOR FLOW MODEL

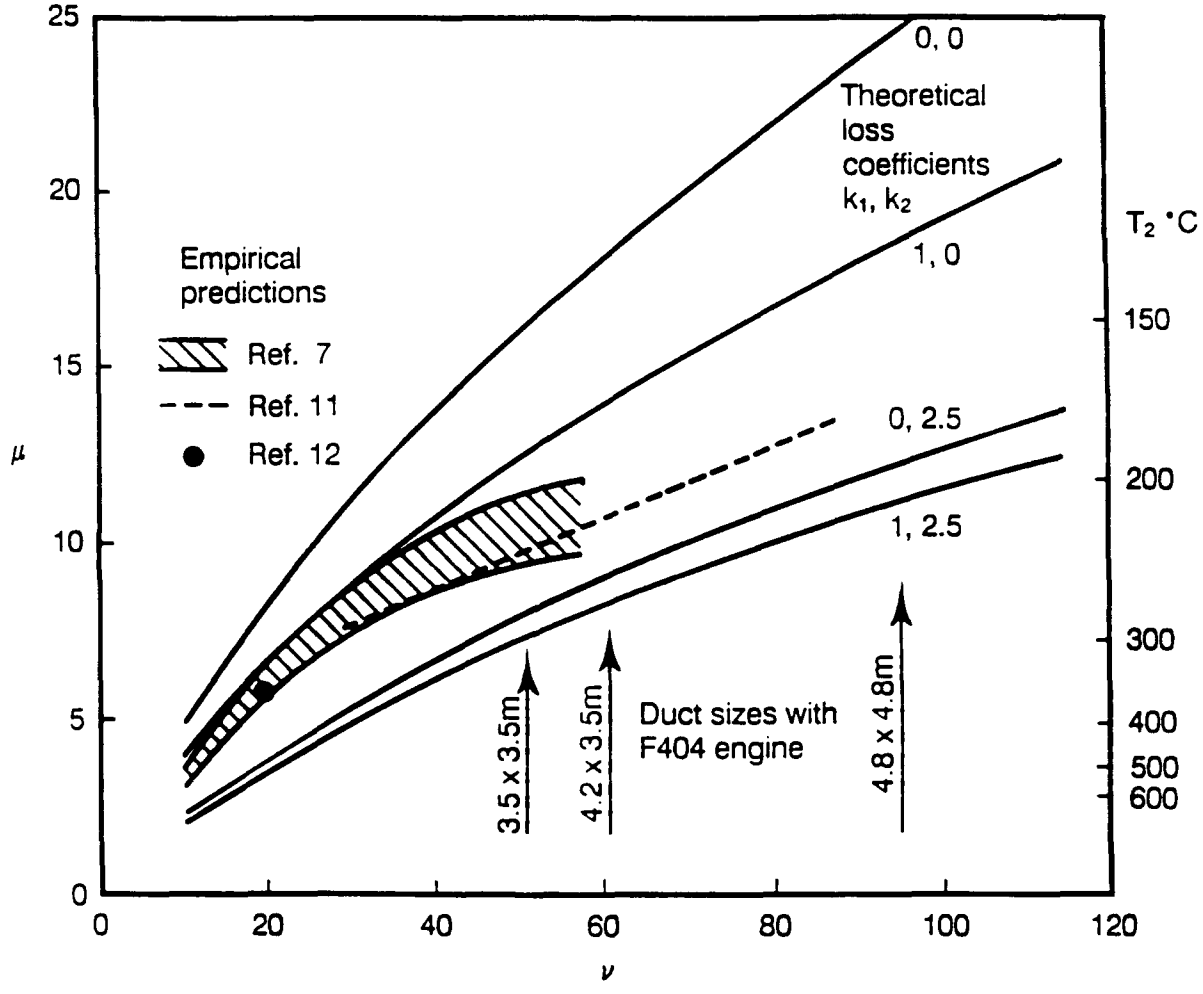


FIGURE 6. AUGMENTOR PUMPING PERFORMANCE - ONE ENGINE MAX A/B

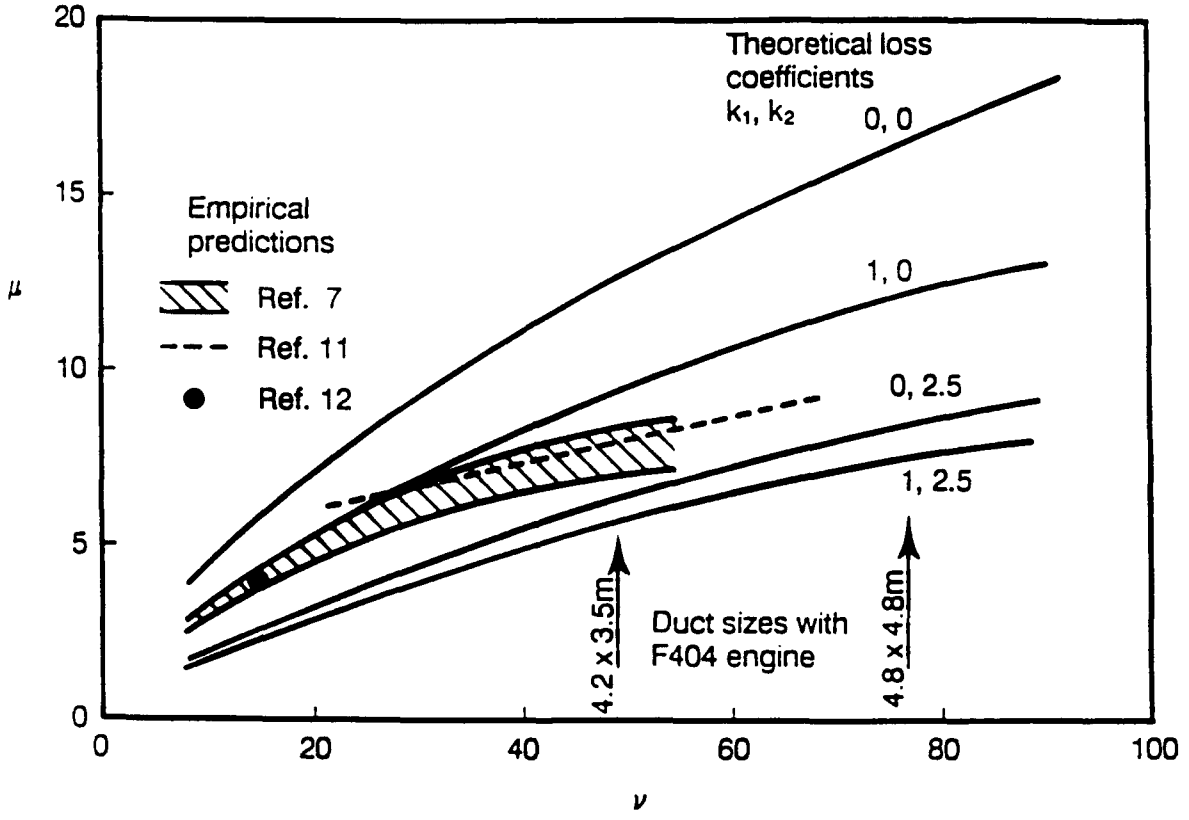


FIGURE 7. AUGMENTOR PUMPING PERFORMANCE - TWO ENGINES IRP

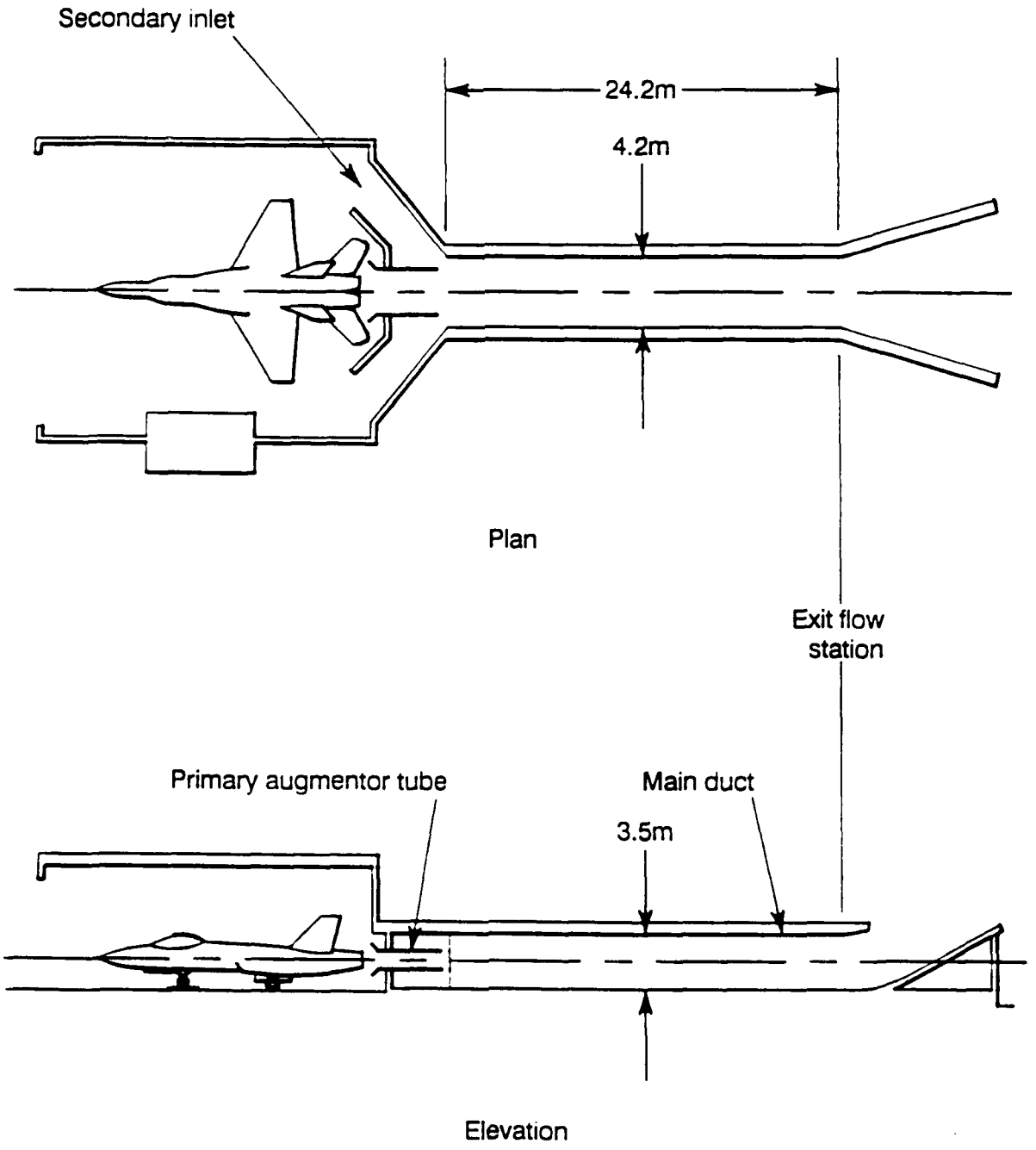


FIGURE 8. INSTALLED ENGINE TEST FACILITY - REVISED DESIGN

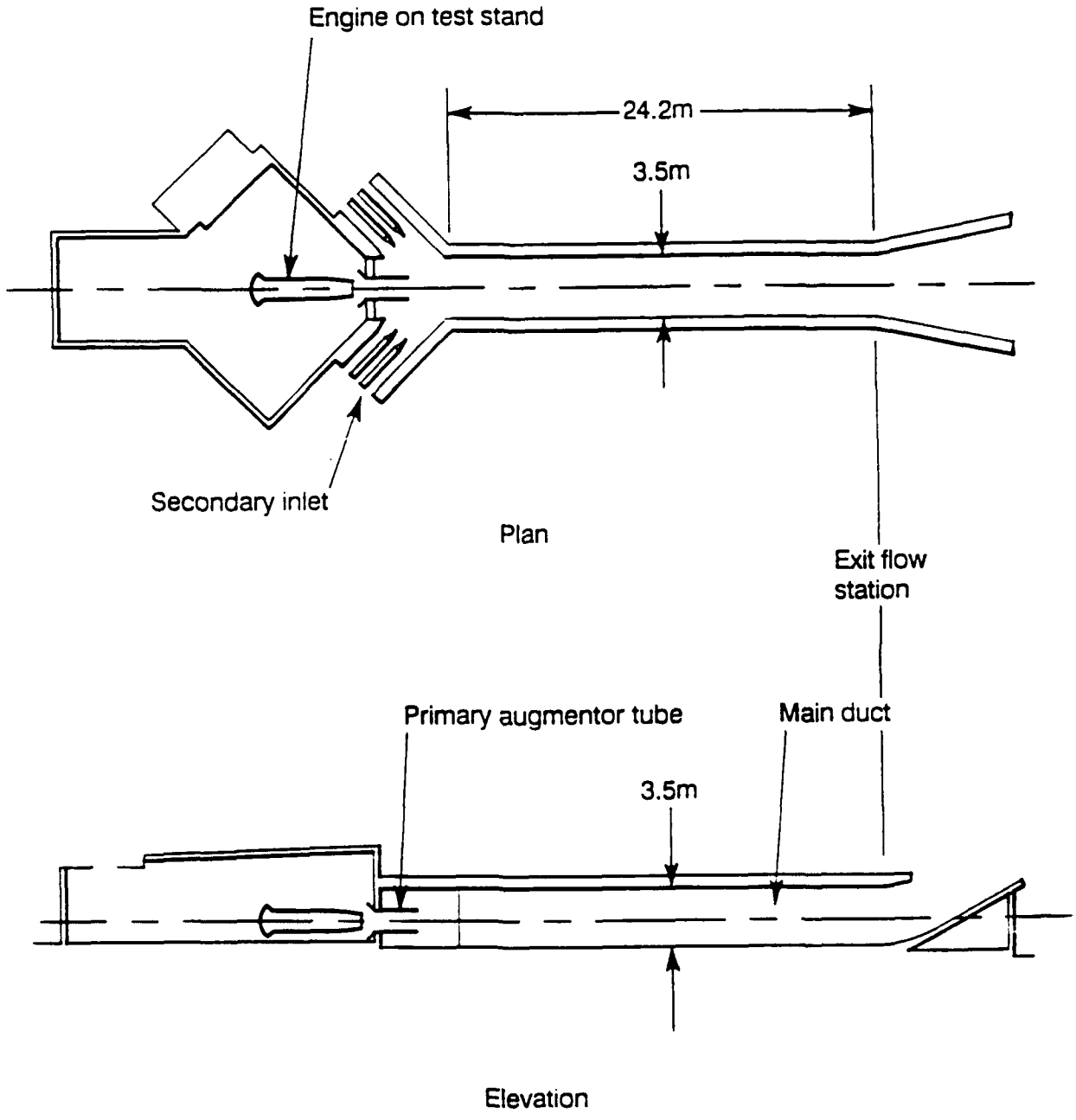


FIGURE 9. UNINSTALLED ENGINE TEST FACILITY - REVISED DESIGN

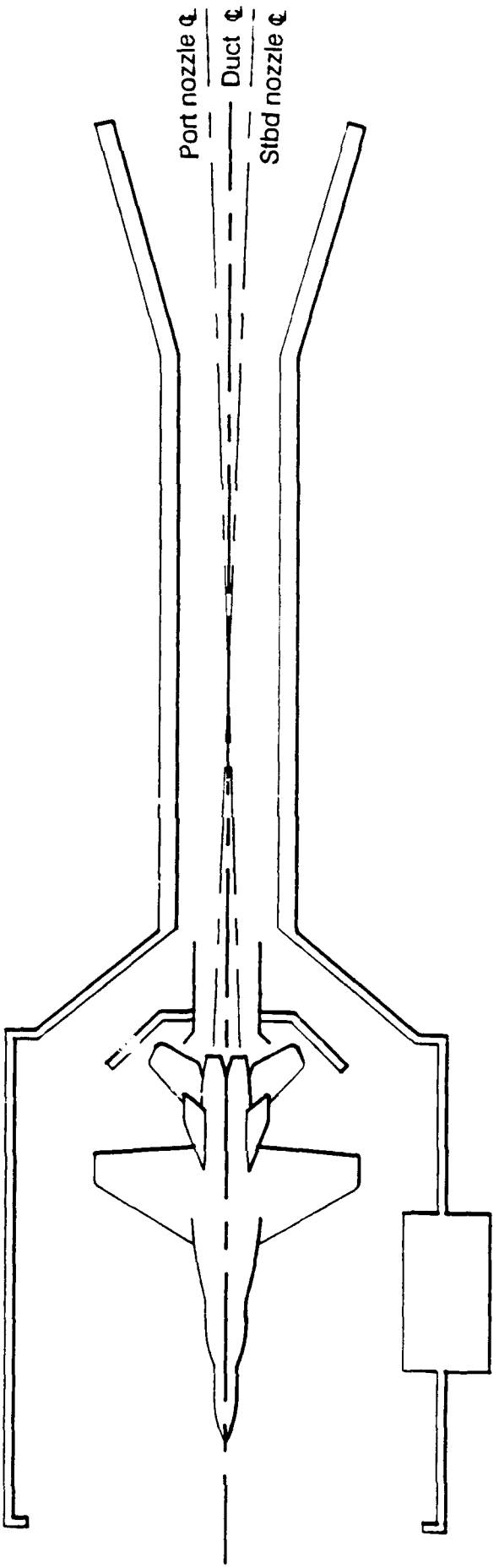


FIGURE 10. JET ALIGNMENT IN INSTALLED ENGINE TEST FACILITY

(a) Installed engine test facility

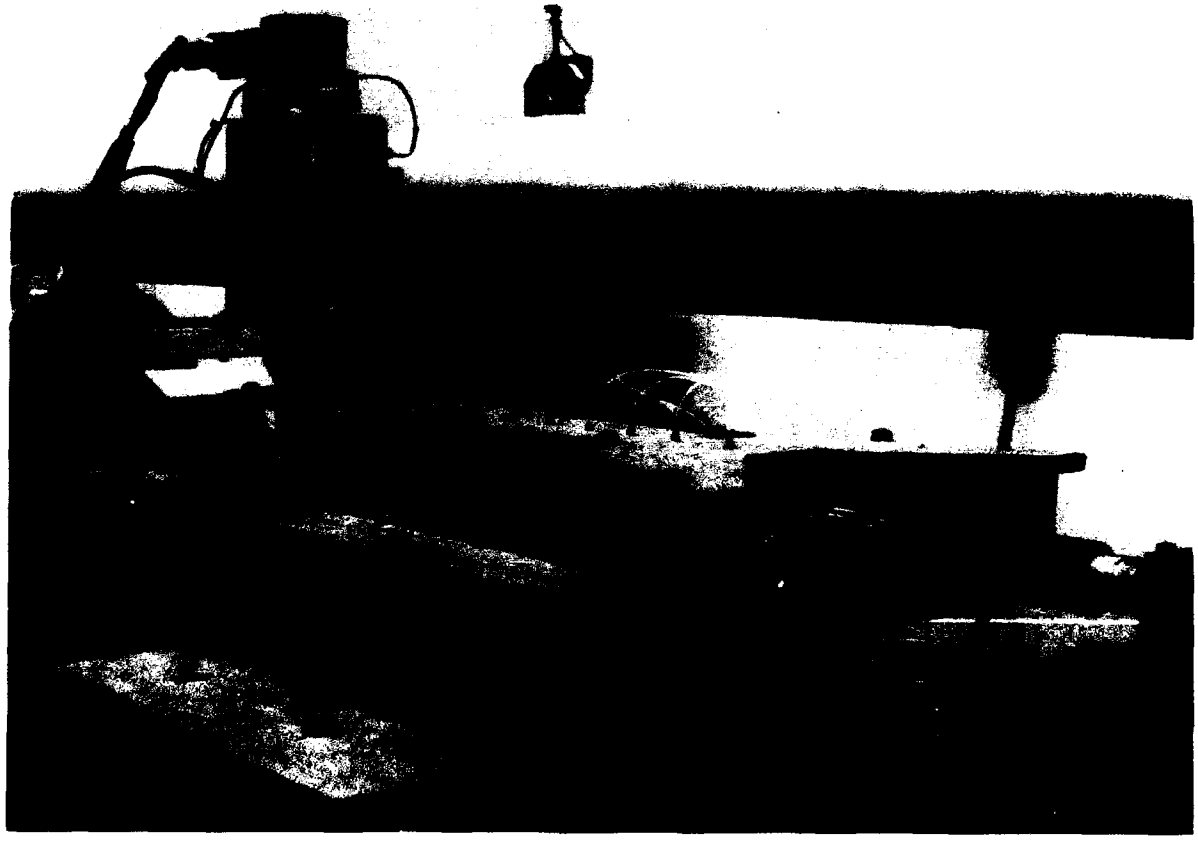

(b) Uninstalled engine test facility

FIGURE 11. PHOTOGRAPHS OF TEST MODELS

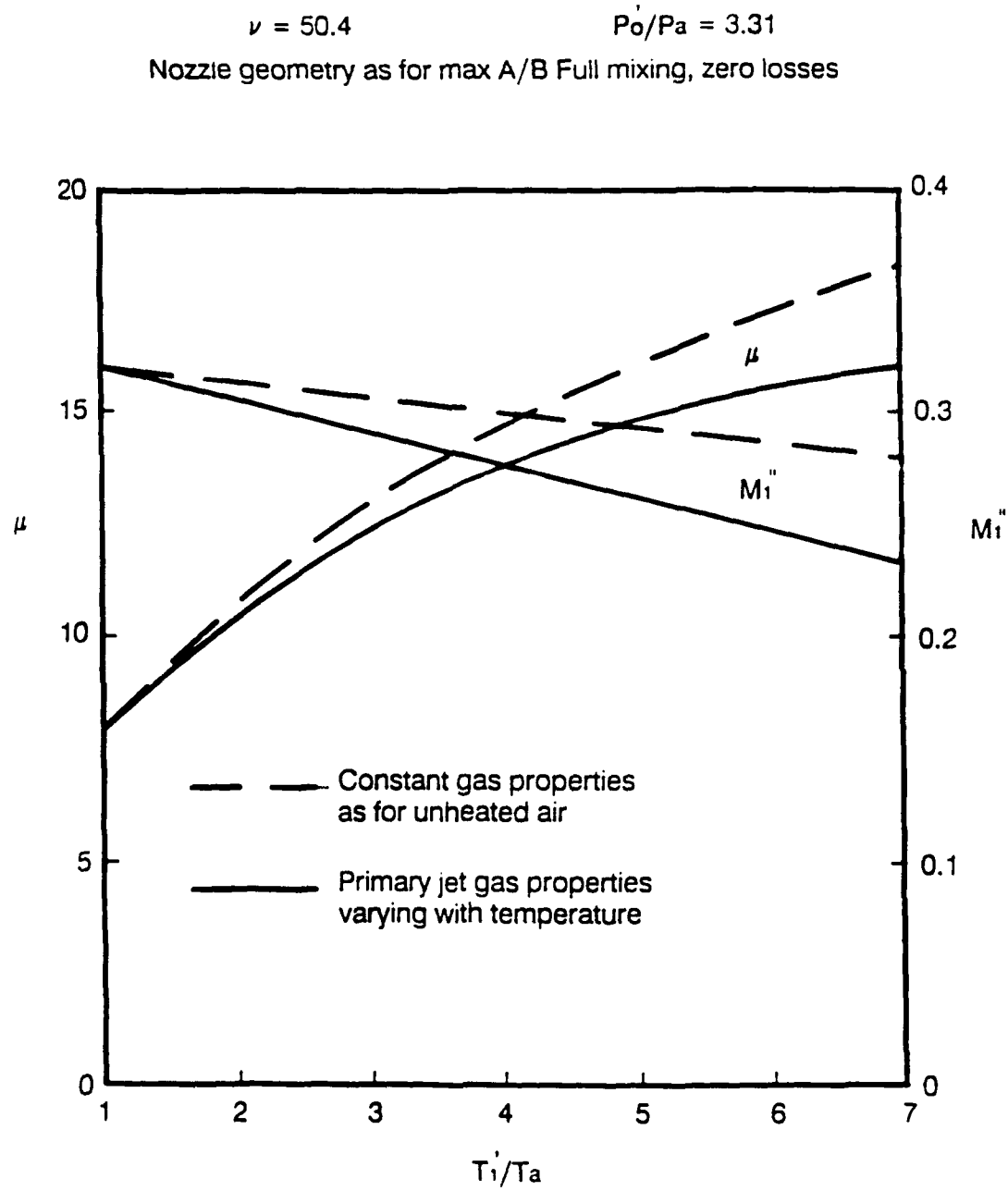


FIGURE 12. THEORETICAL EFFECT OF JET TEMPERATURE AND GAS PROPERTIES

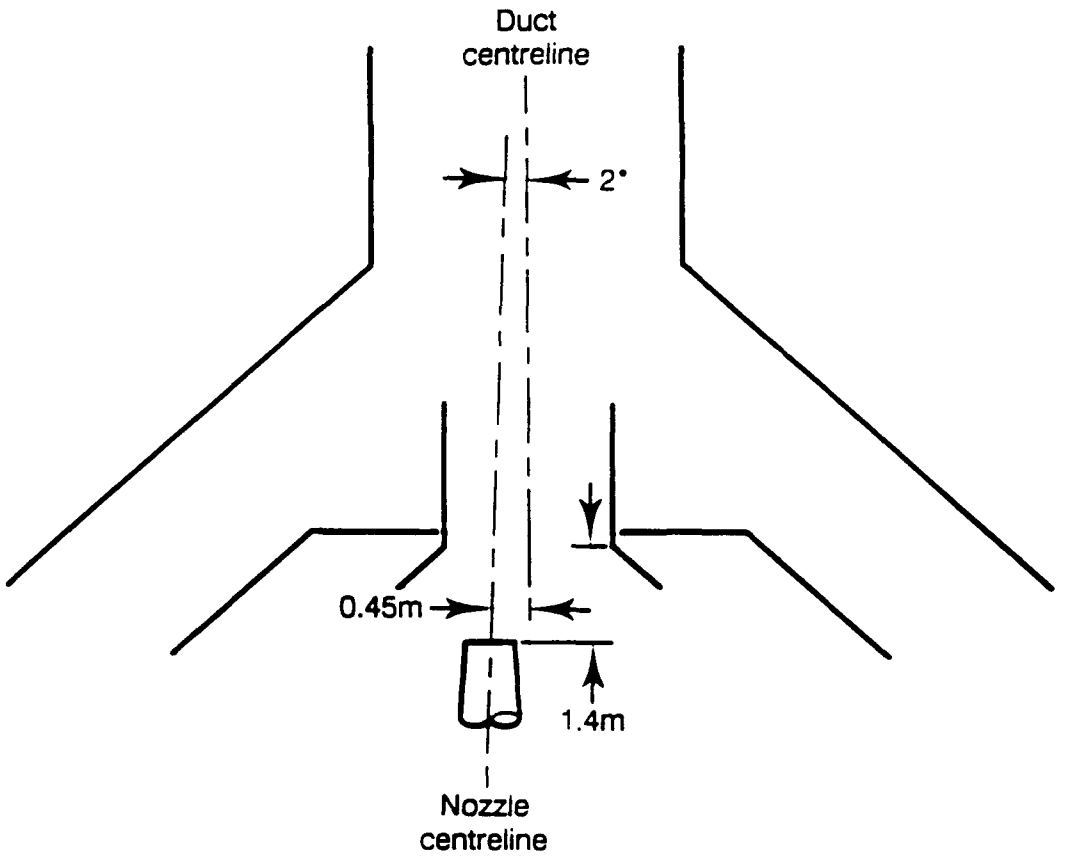


FIGURE 13. NOZZLE ALIGNMENT IN INSTALLED ENGINE MODEL

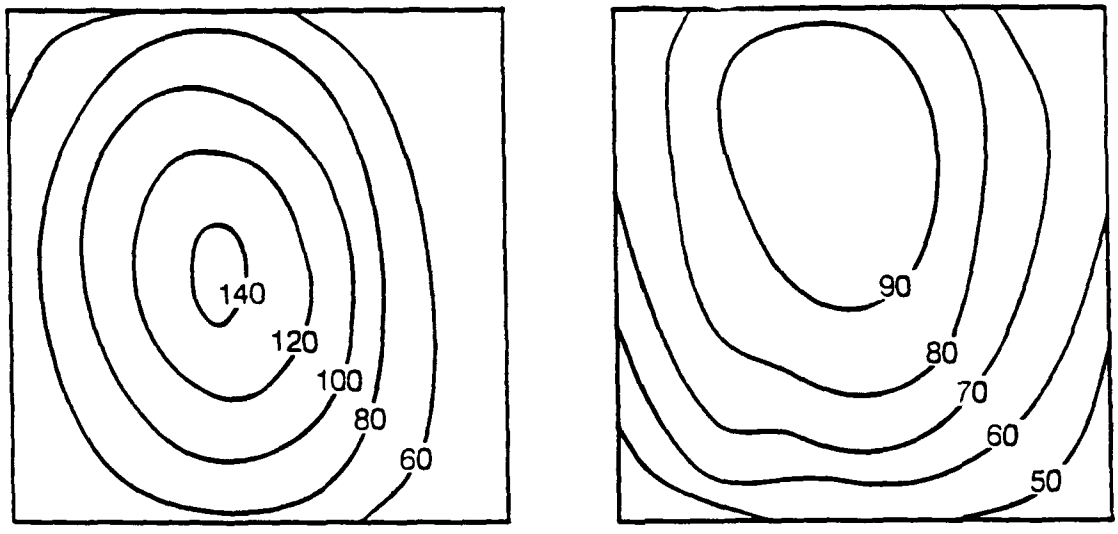


Intermediate flow station

Duct exit plane

(a) Ramp in position $\mu = 4.58$

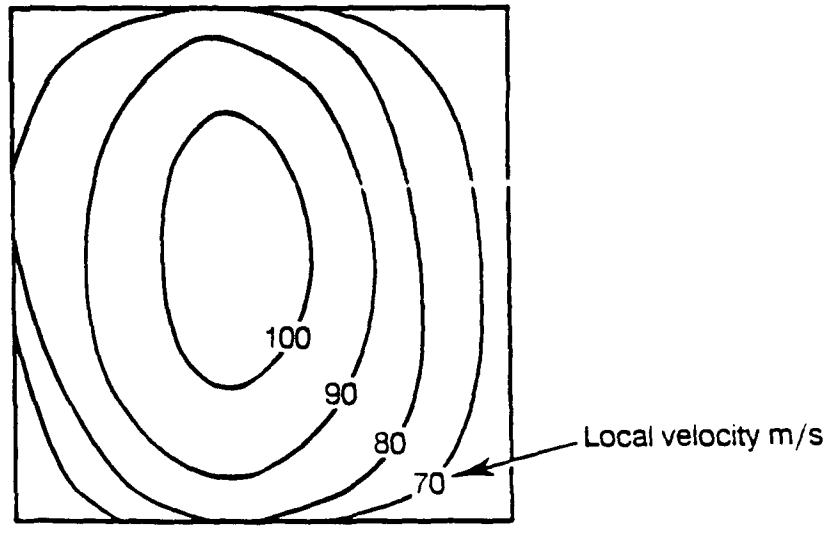


Duct exit plane

(b) Ramp removed $\mu = 5.28$

FIGURE 14. EFFECT OF DEFLECTOR RAMP ON DUCT VELOCITY DISTRIBUTION - UNINSTALLED ENGINE FACILITY

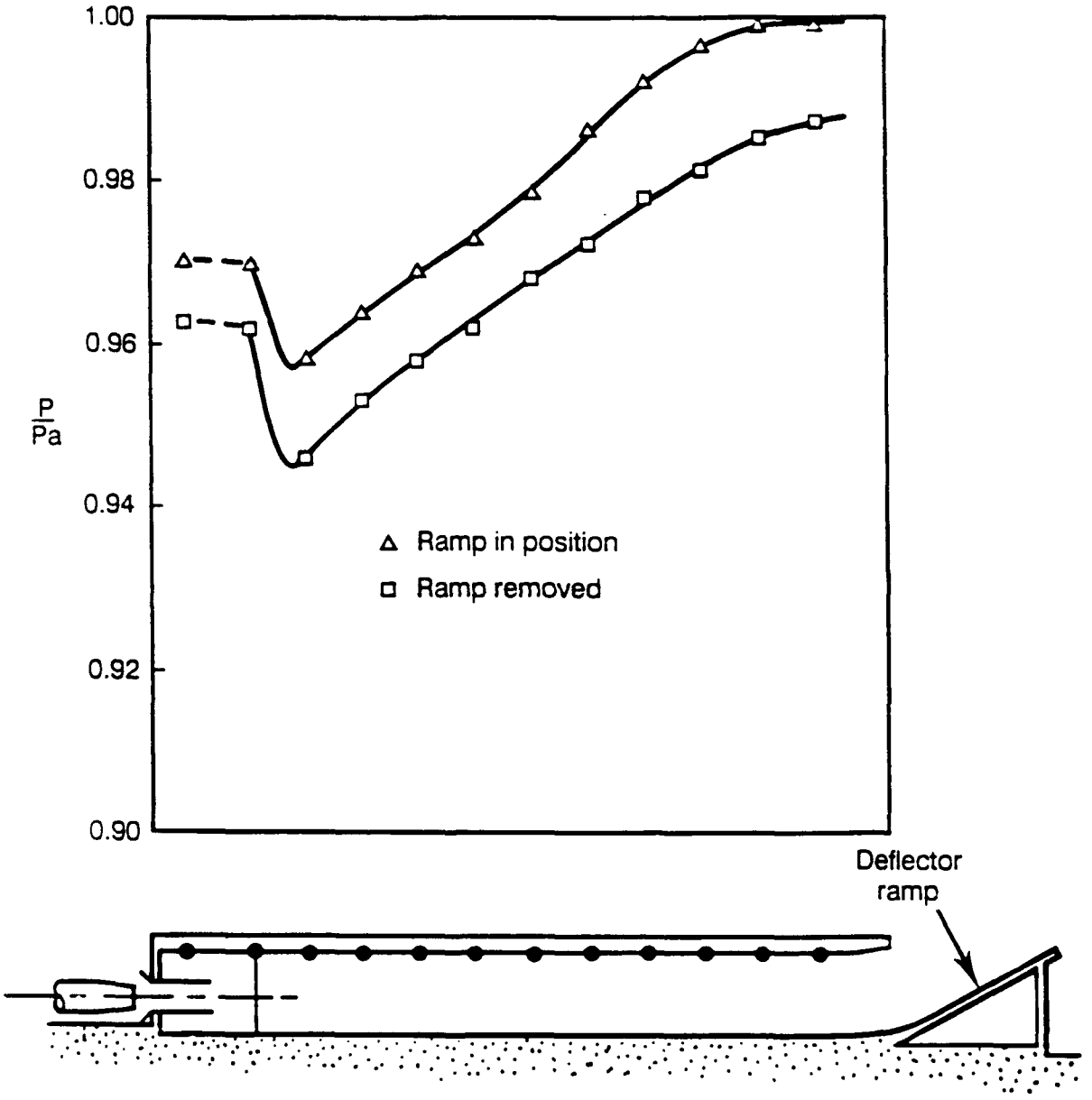


FIGURE 15. EFFECT OF DEFLECTOR RAMP ON STATIC PRESSURE DISTRIBUTION - UNINSTALLED ENGINE FACILITY

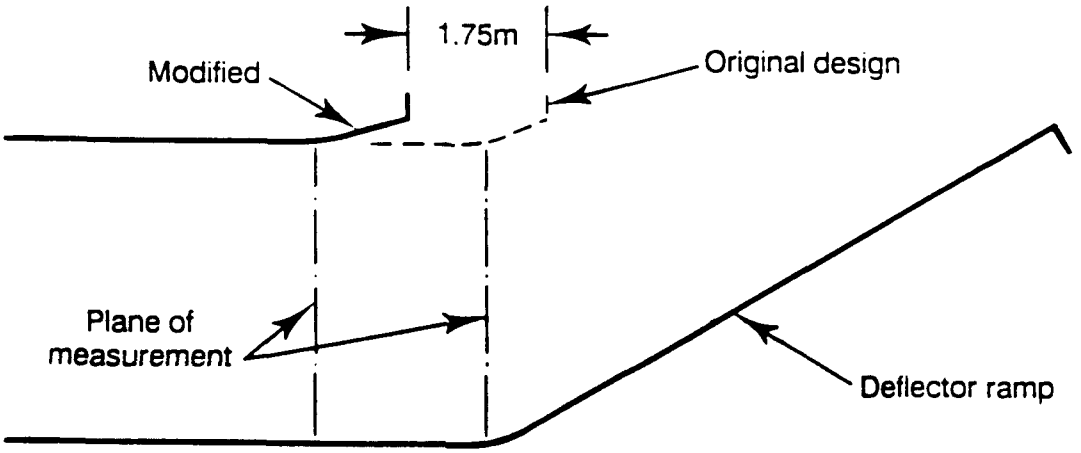


FIGURE 16. MODIFICATION AT DUCT EXIT

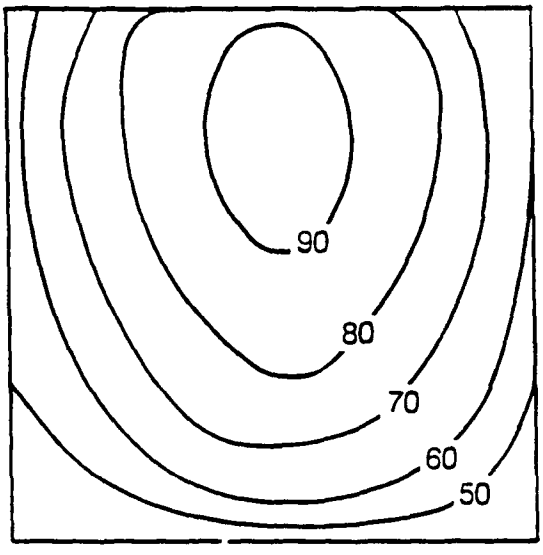


Original design
$\mu$ = 4.30

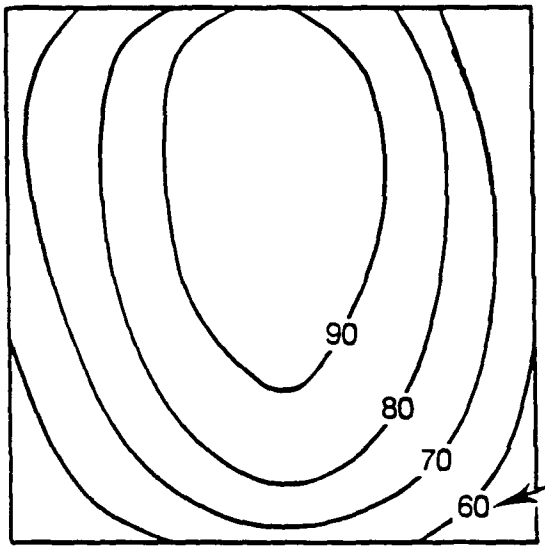


Modified design
$\mu$ = 4.88

Local velocity m/s

FIGURE 17. EFFECT OF RAMP POSITION ON EXIT VELOCITY DISTRIBUTION - UNINSTALLED ENGINE FACILITY

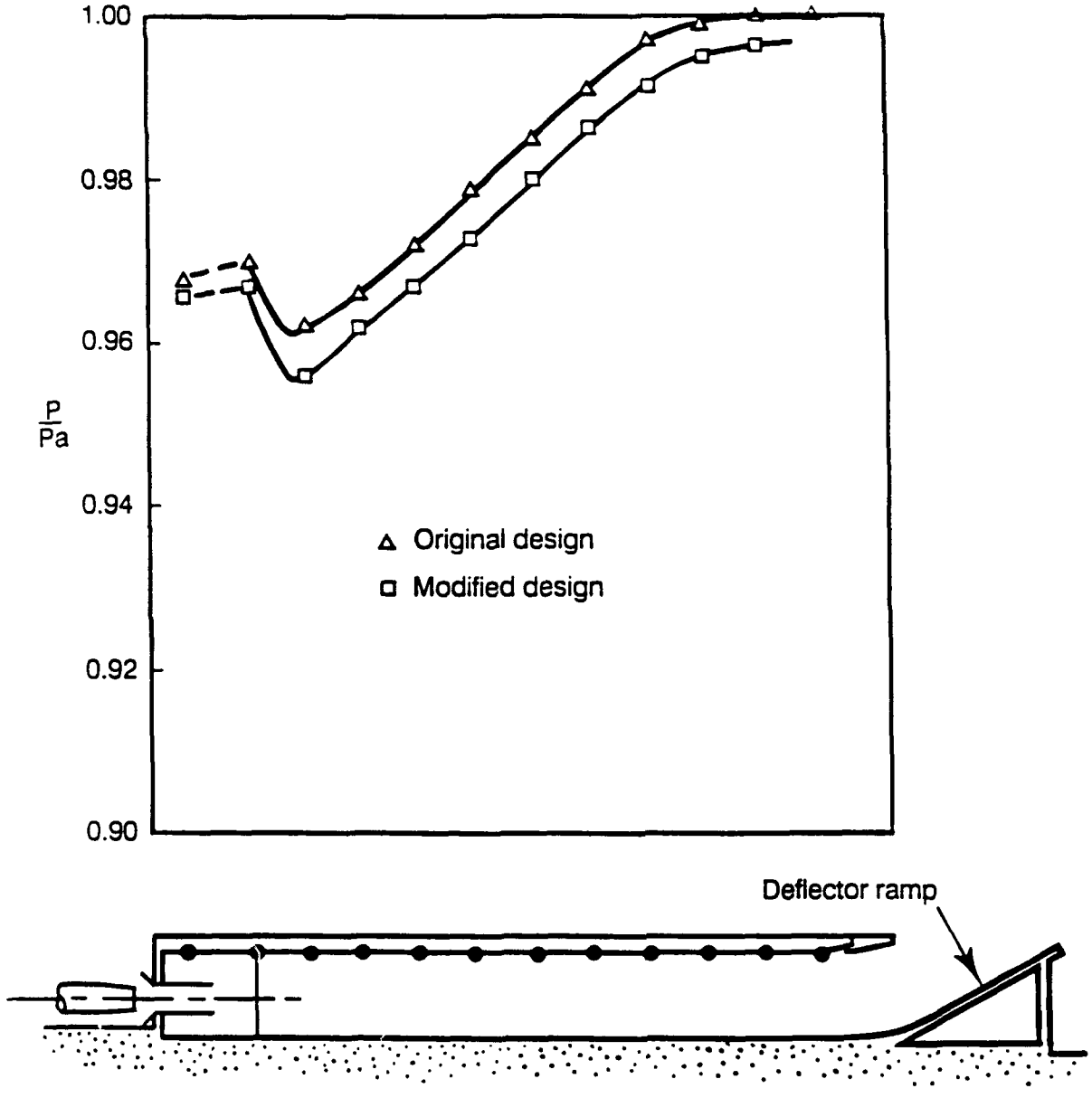


FIGURE 18. EFFECT OF RAMP POSITION ON STATIC PRESSURE DISTRIBUTION - UNINSTALLED ENGINE FACILITY

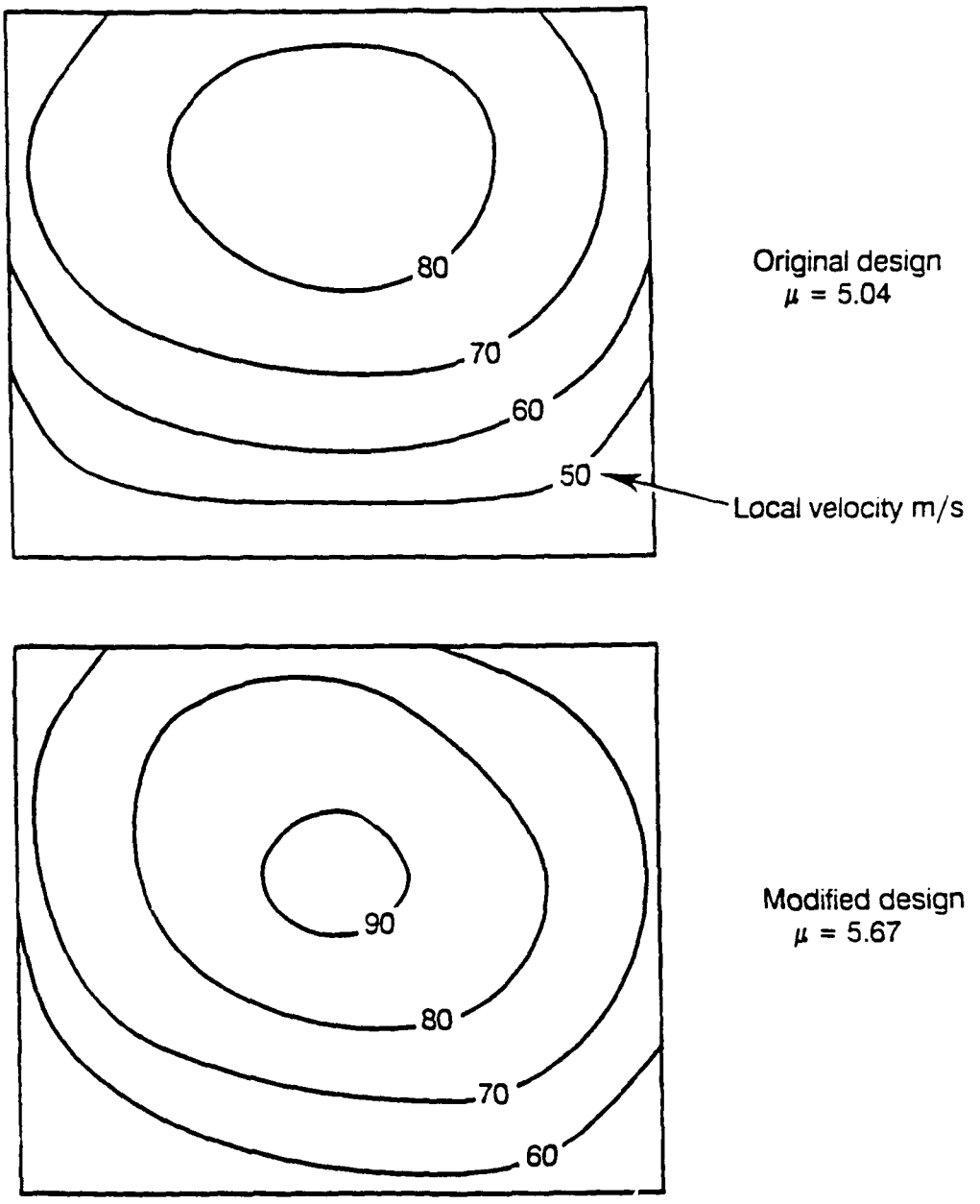


FIGURE 19. EFFECT OF RAMP POSITION ON EXIT VELOCITY DISTRIBUTION - INSTALLED ENGINE FACILITY

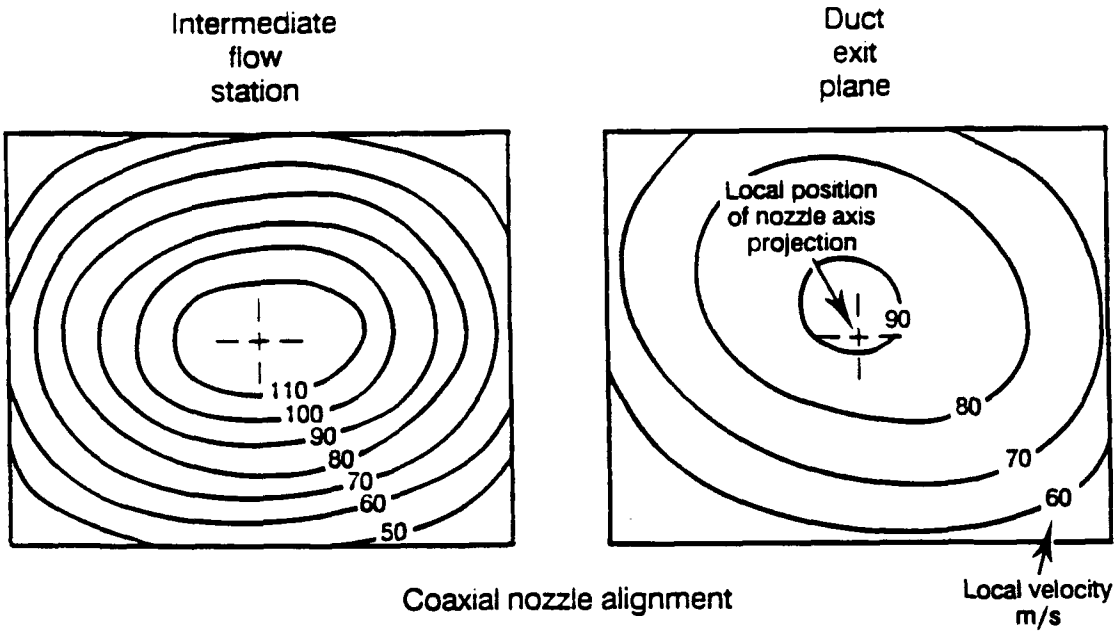


FIGURE 20. EFFECT OF JET ALIGNMENT ON DUCT VELOCITY DISTRIBUTION WITH ORIGINAL PRIMARY TUBE DESIGN, w = 2.2m h = 1.3m l = 2.0m - INSTALLED ENGINE TEST FACILITY

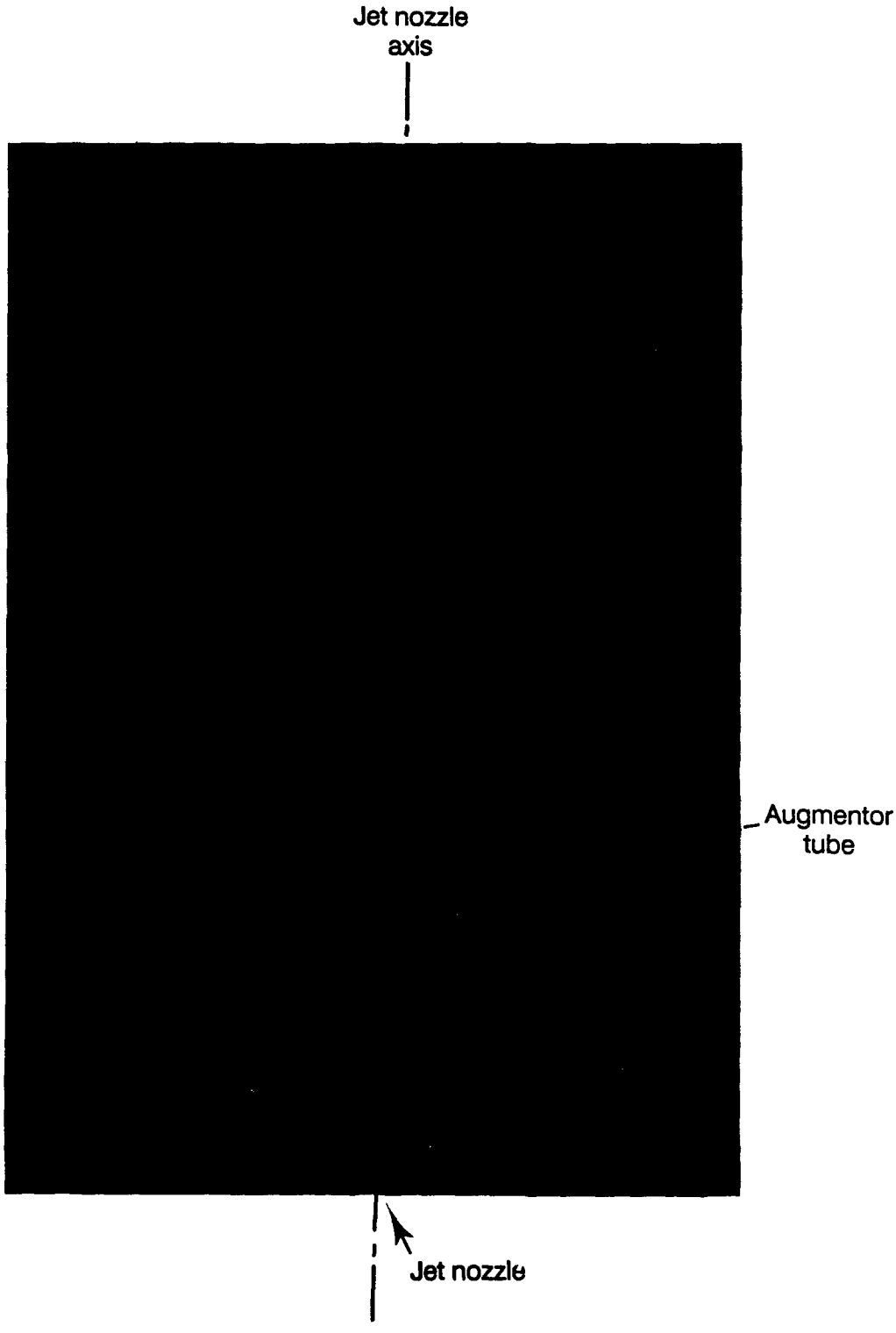


FIGURE 21. SCHLIEREN PHOTOGRAPH OF JET WITH PRIMARY TUBE IN ISOLATION

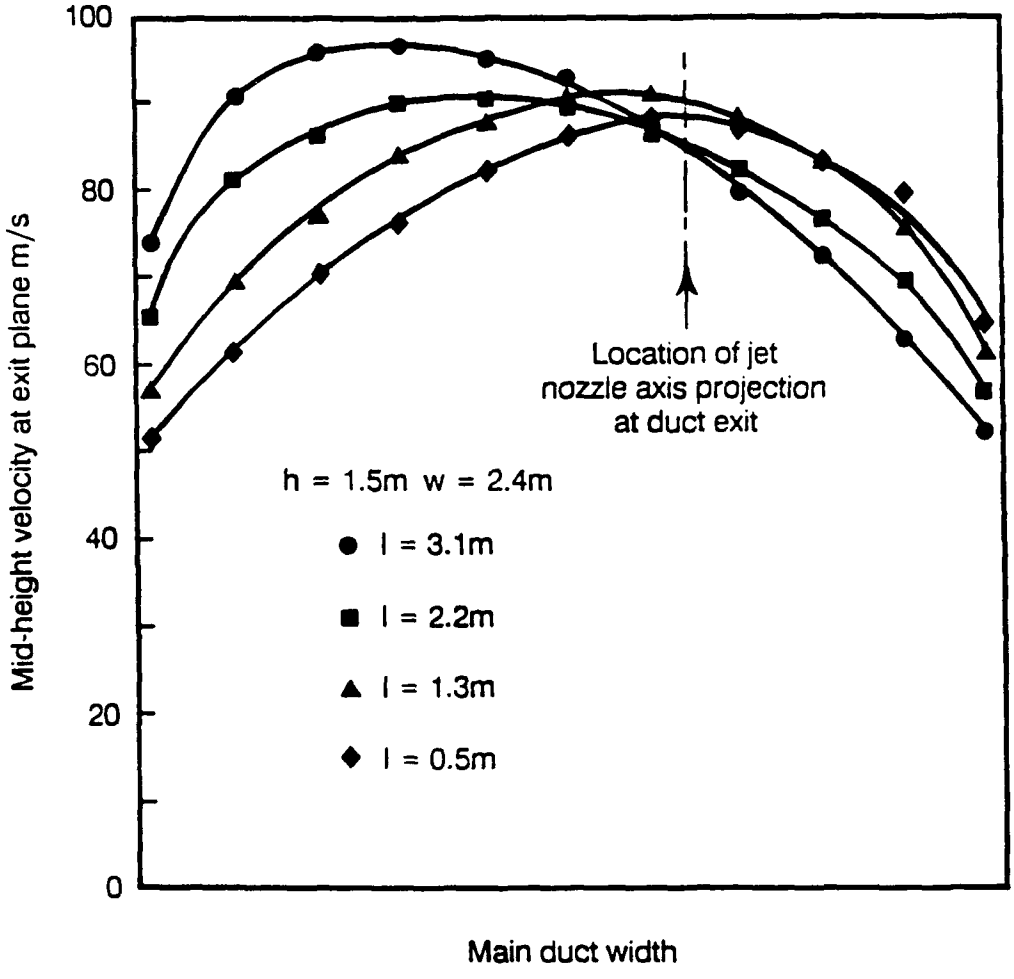


FIGURE 22. EFFECT OF PRIMARY TUBE LENGTH ON LATERAL VELOCITY PROFILE - INSTALLED ENGINE FACILITY

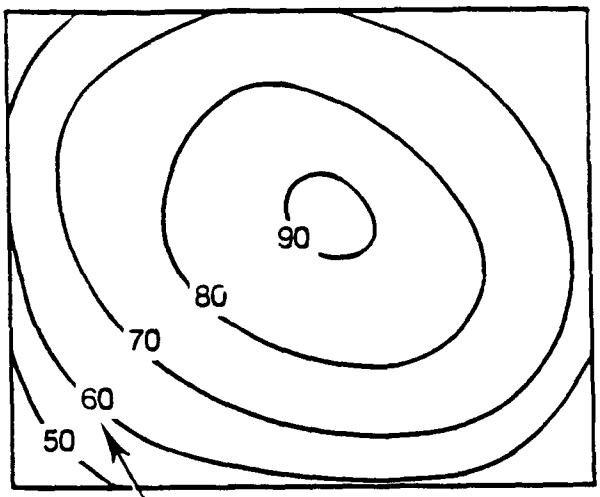


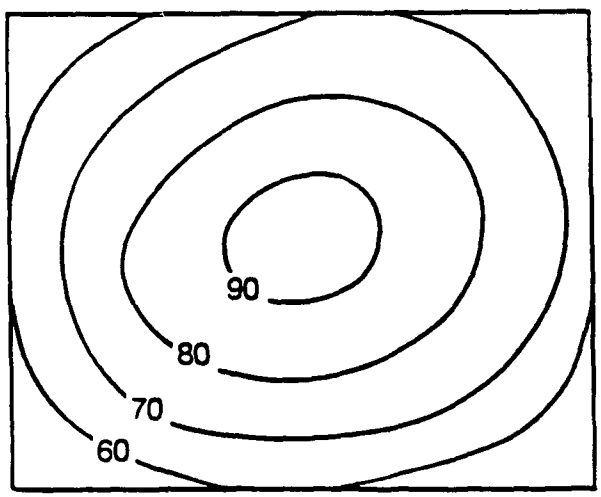


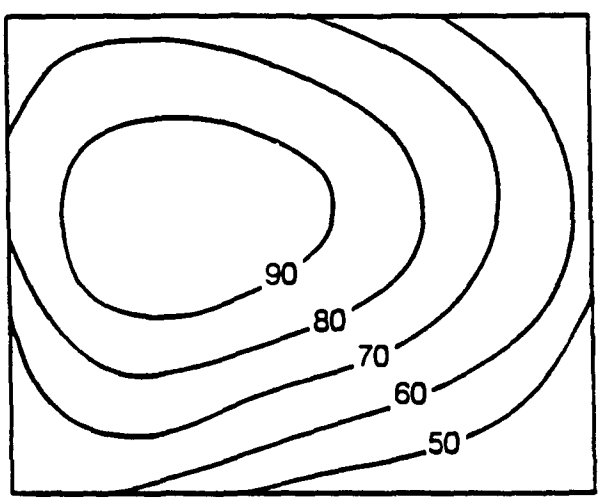


FIGURE 23. EFFECT OF PRIMARY TUBE LENGTH ON EXIT VELOCITY DISTRIBUTION - INSTALLED ENGINE FACILITY

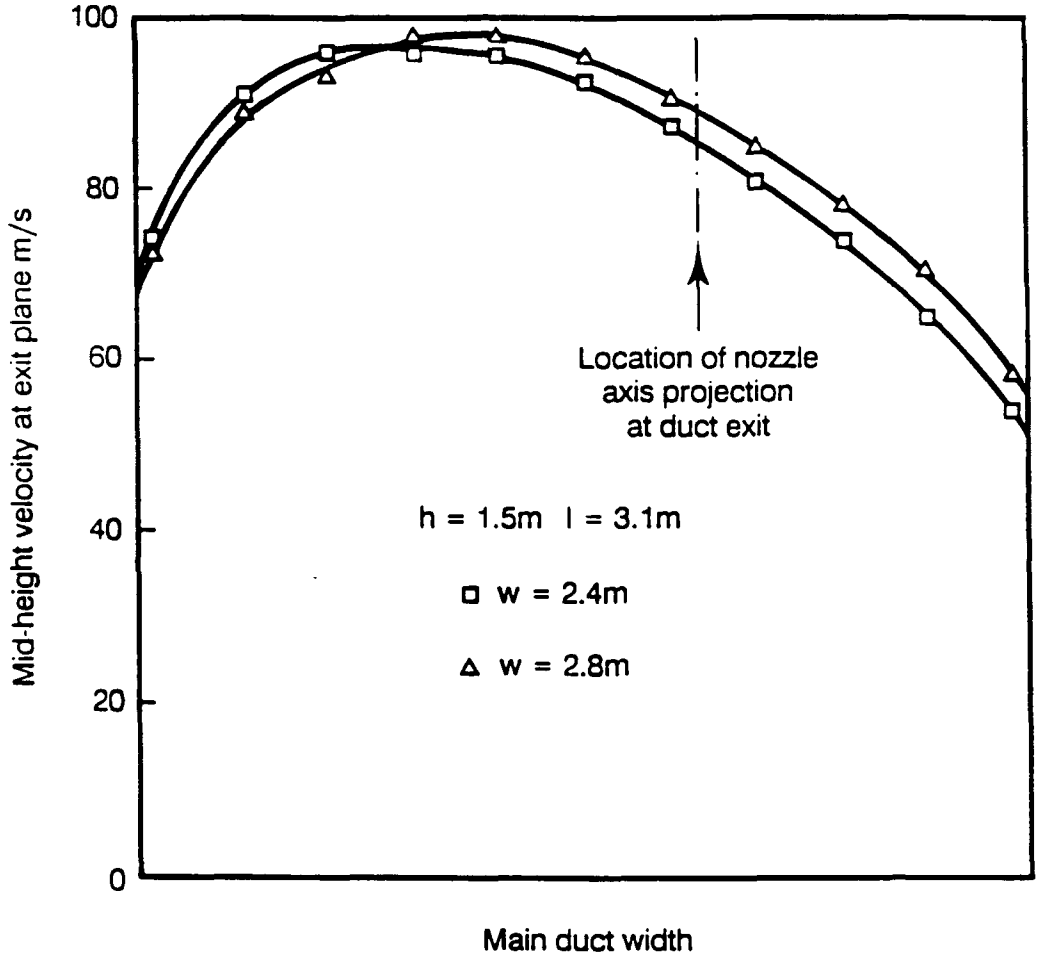


FIGURE 24. EFFECT OF PRIMARY TUBE WIDTH ON LATERAL VELOCITY PROFILE - INSTALLED ENGINE FACILITY

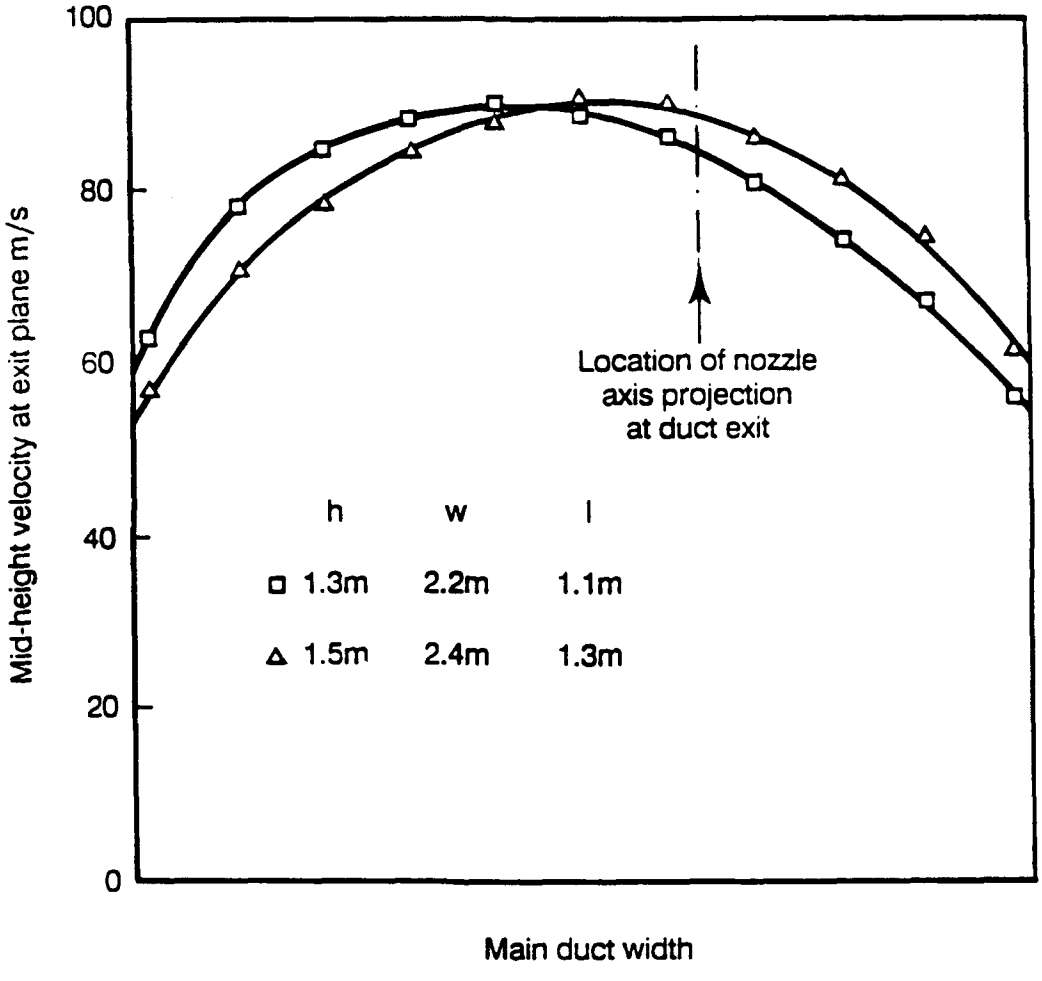


FIGURE 25. EFFECT OF PRIMARY TUBE SCALE ON LATERAL VELOCITY PROFILE - INSTALLED ENGINE FACILITY

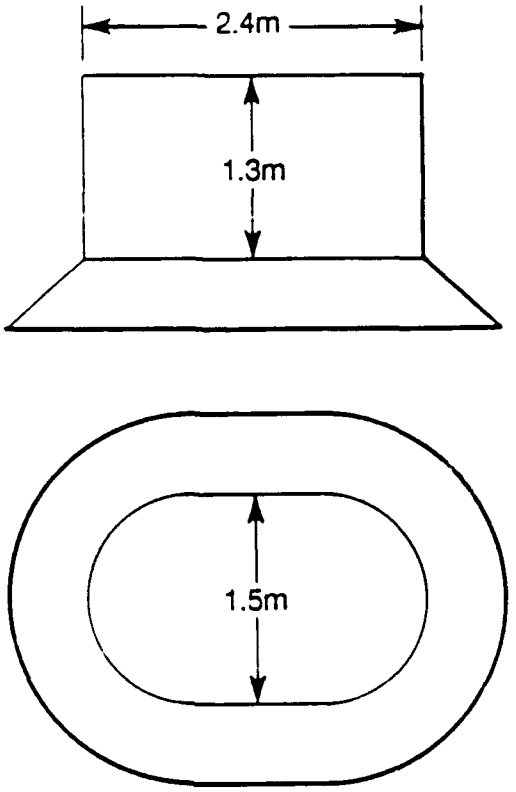


(a) Installed engine facility

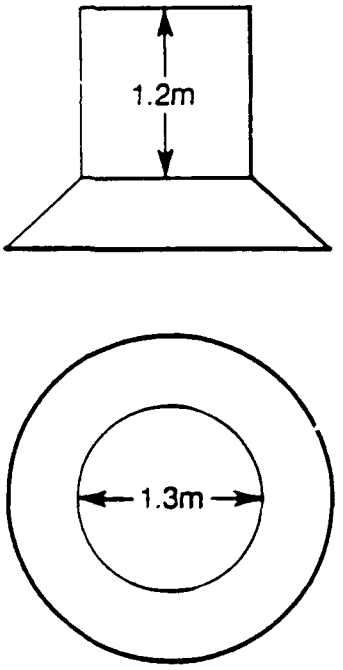


(b) Uninstalled engine facility

FIGURE 26. ADOPTED PRIMARY TUBE DIMENSIONS

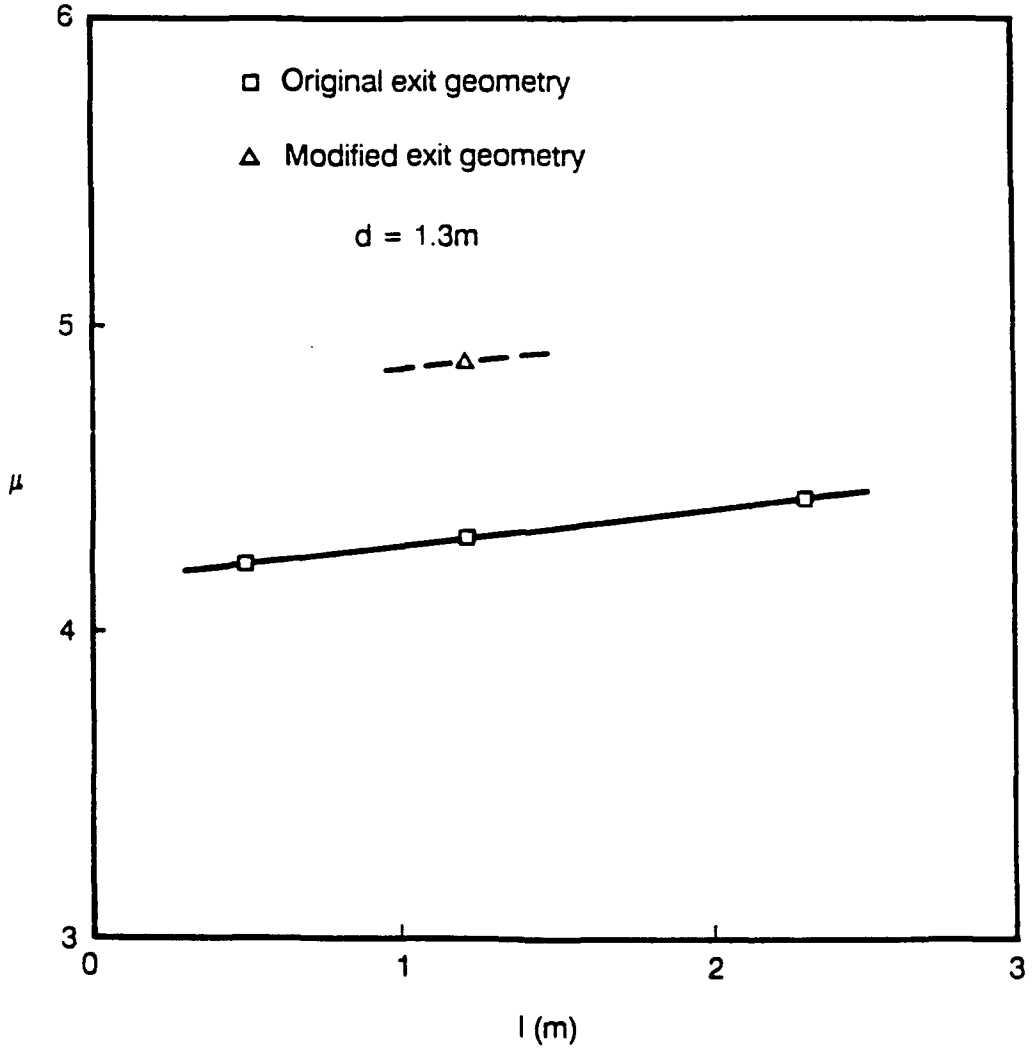


FIGURE 27. EFFECT OF PRIMARY TUBE LENGTH ON AUGMENTATION RATIO - UNINSTALLED ENGINE FACILITY

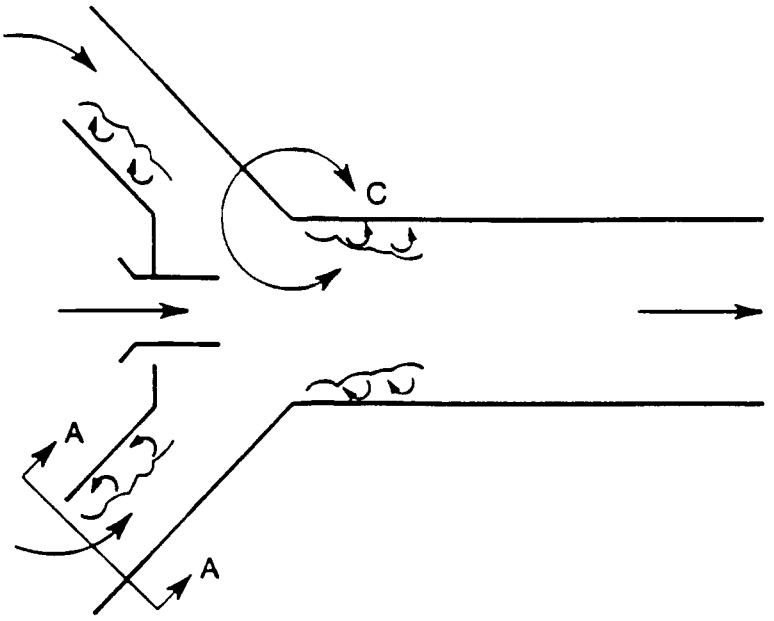


(a) Flow separations in unmodified design

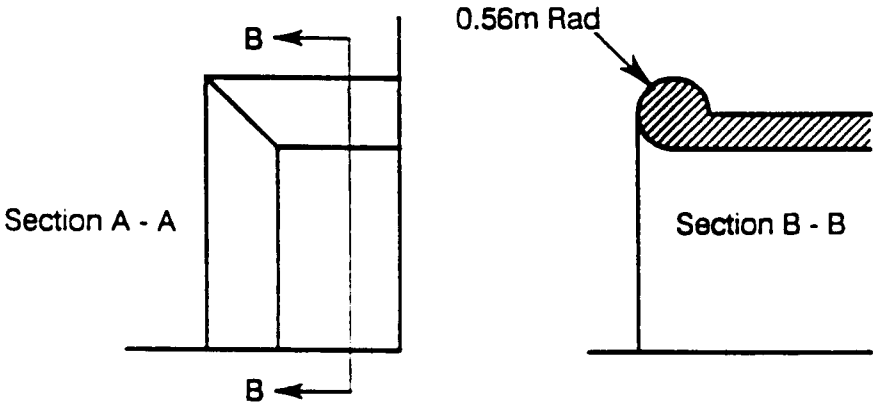


(b) Bellmouth fairings

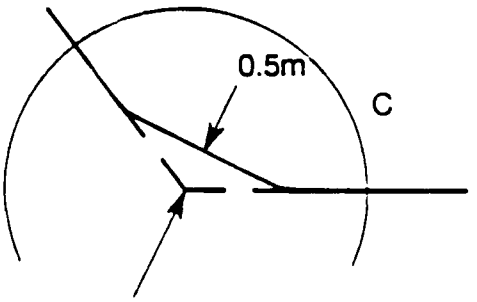


(c) Duct corner fairings

FIGURE 28. INLET MODIFICATIONS - INSTALLED ENGINE FACILITY

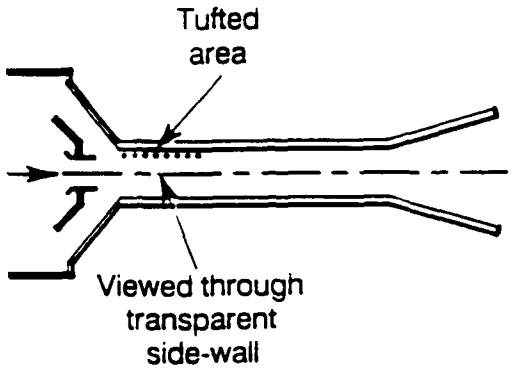


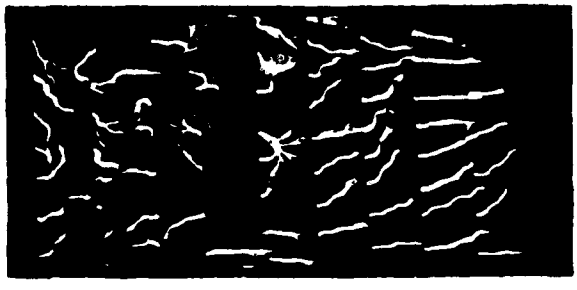

(a) No fairings

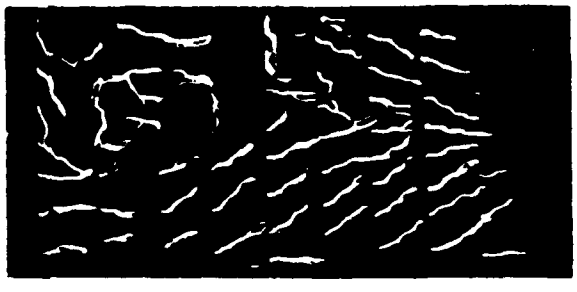

(b) Inlet bellmouths fitted

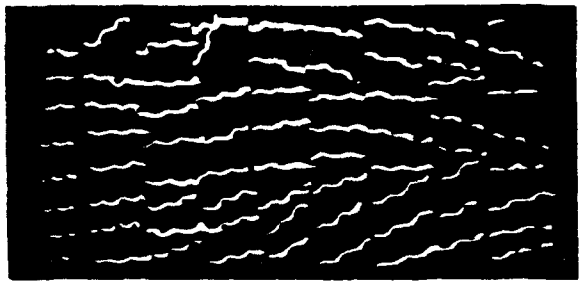

(c) Inlet bellmouths and faired duct corners

FIGURE 29. SURFACE FLOW VISUALISATION IN AUGMENTOR DUCT - INSTALLED ENGINE FACILITY

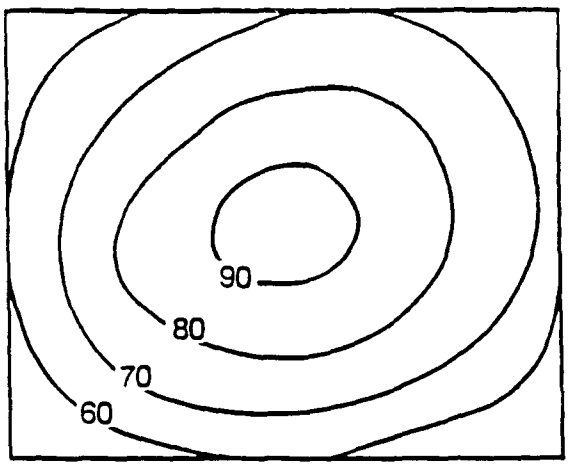


(a)
No fairings
$\mu$ = 5.59

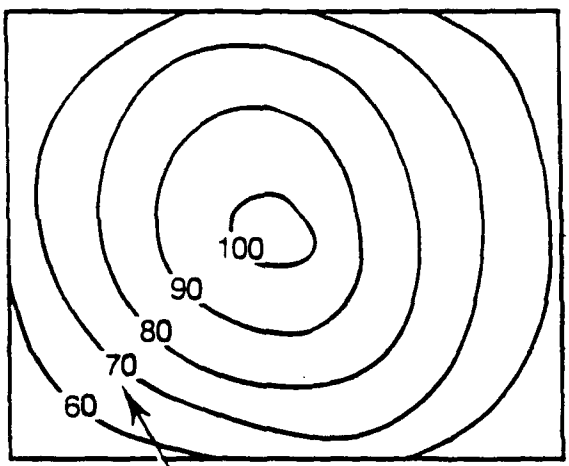


(b)
Inlet bellmouths fitted
$\mu$ = 5.74

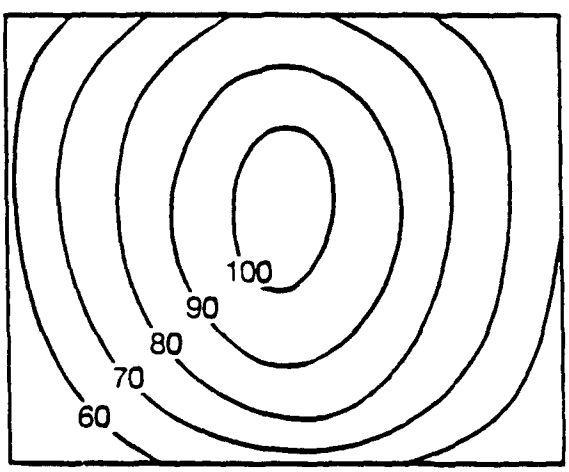


(c)
Inlet bellmouths and faired
duct corners
$\mu$ = 5.99

FIGURE 30. EFFECT OF INLET MODIFICATIONS ON EXIT VELOCITY DISTRIBUTION - INSTALLED ENGINE FACILITY

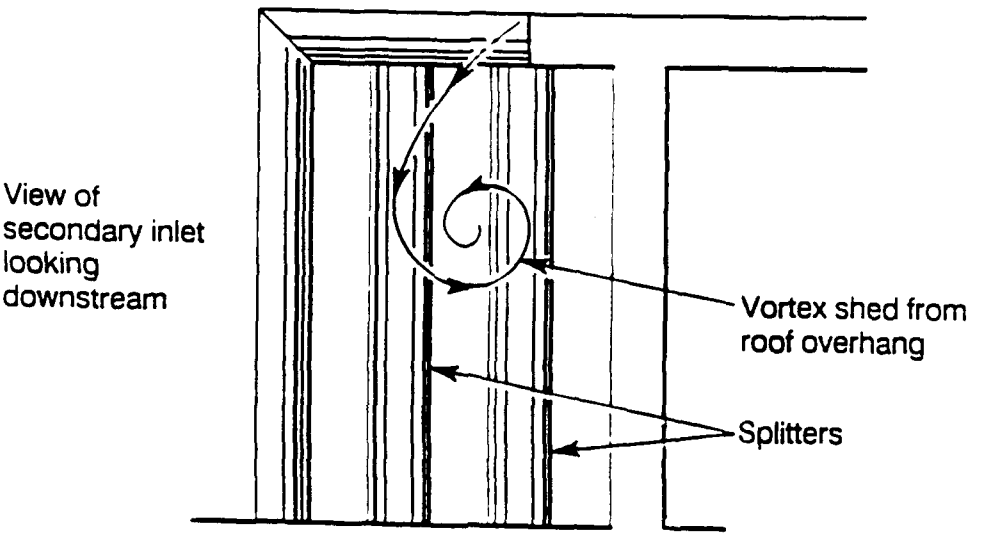


Unmodified

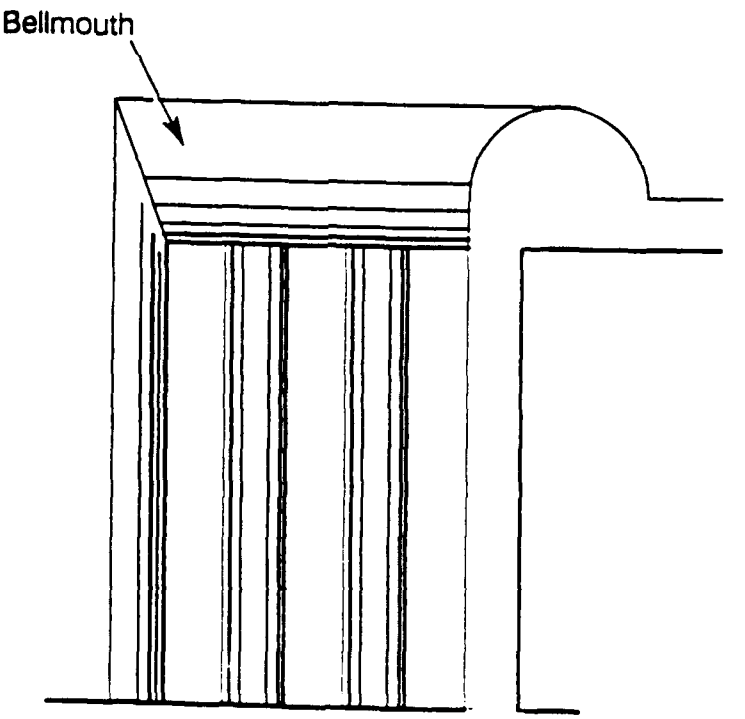


Modified

FIGURE 31. INLET MODIFICATION - UNINSTALLED ENGINE FACILITY

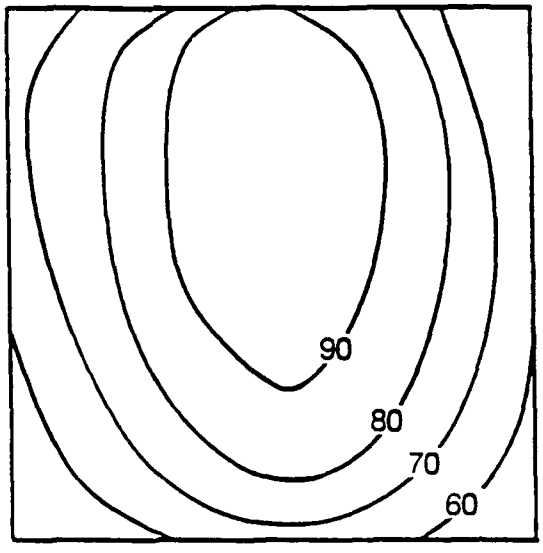


(a)
Unmodified inlet
$\mu$ = 4.88

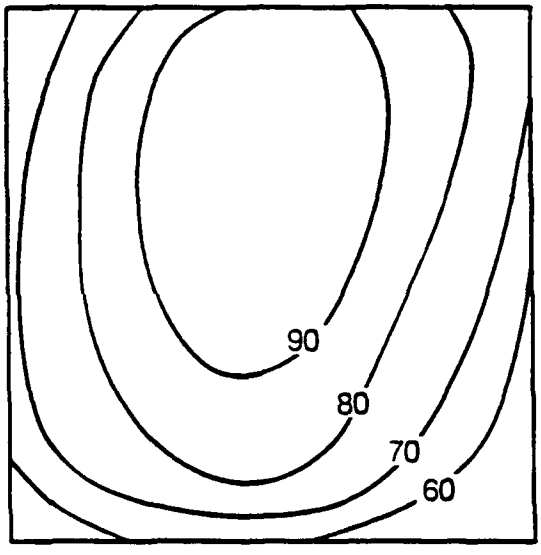


(b)
Modified inlet
$\mu$ = 4.97

FIGURE 32. EFFECT OF INLET MODIFICATIONS ON EXIT VELOCITY DISTRIBUTION - UNINSTALLED ENGINE FACILITY

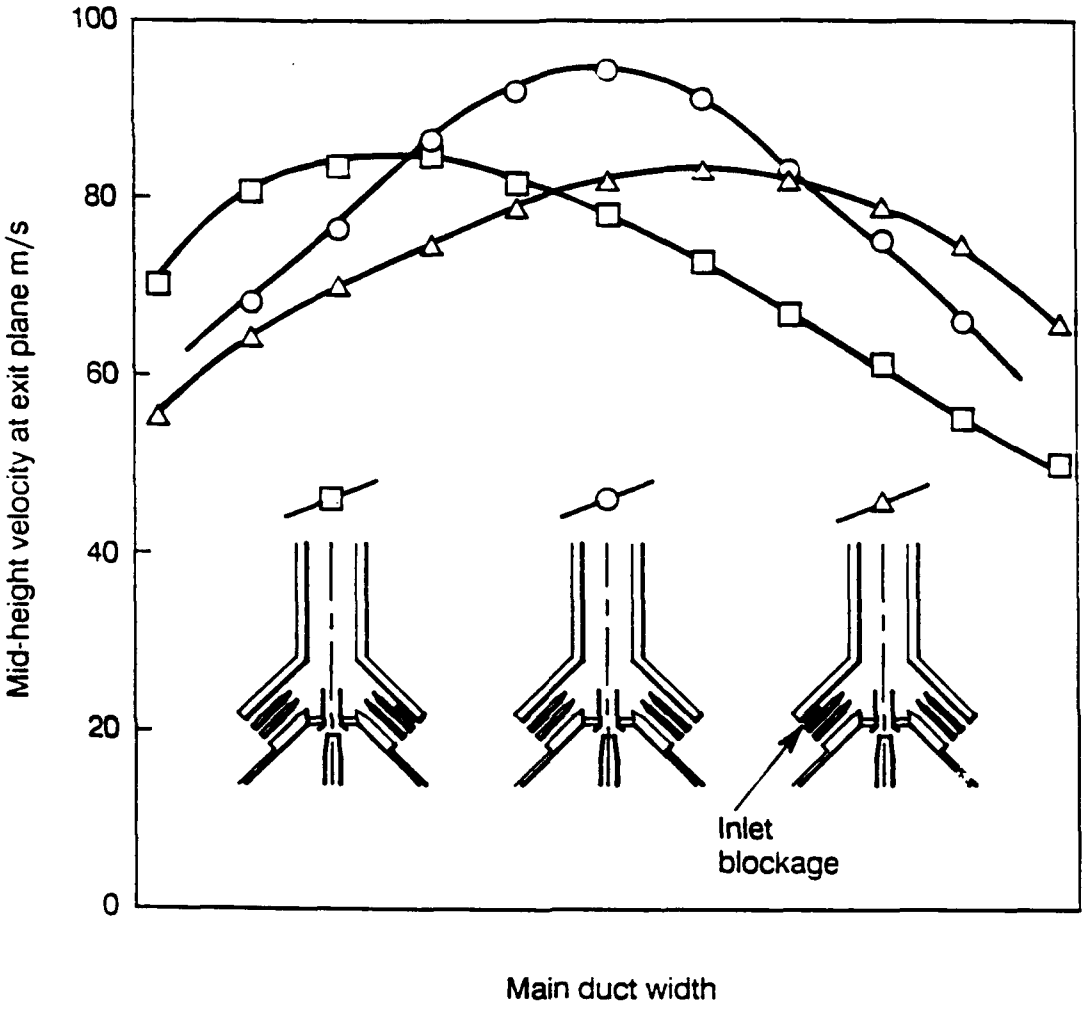


FIGURE 33. EFFECT OF INLET BLOCKAGE ON LATERAL VELOCITY PROFILE - UNINSTALLED ENGINE FACILITY

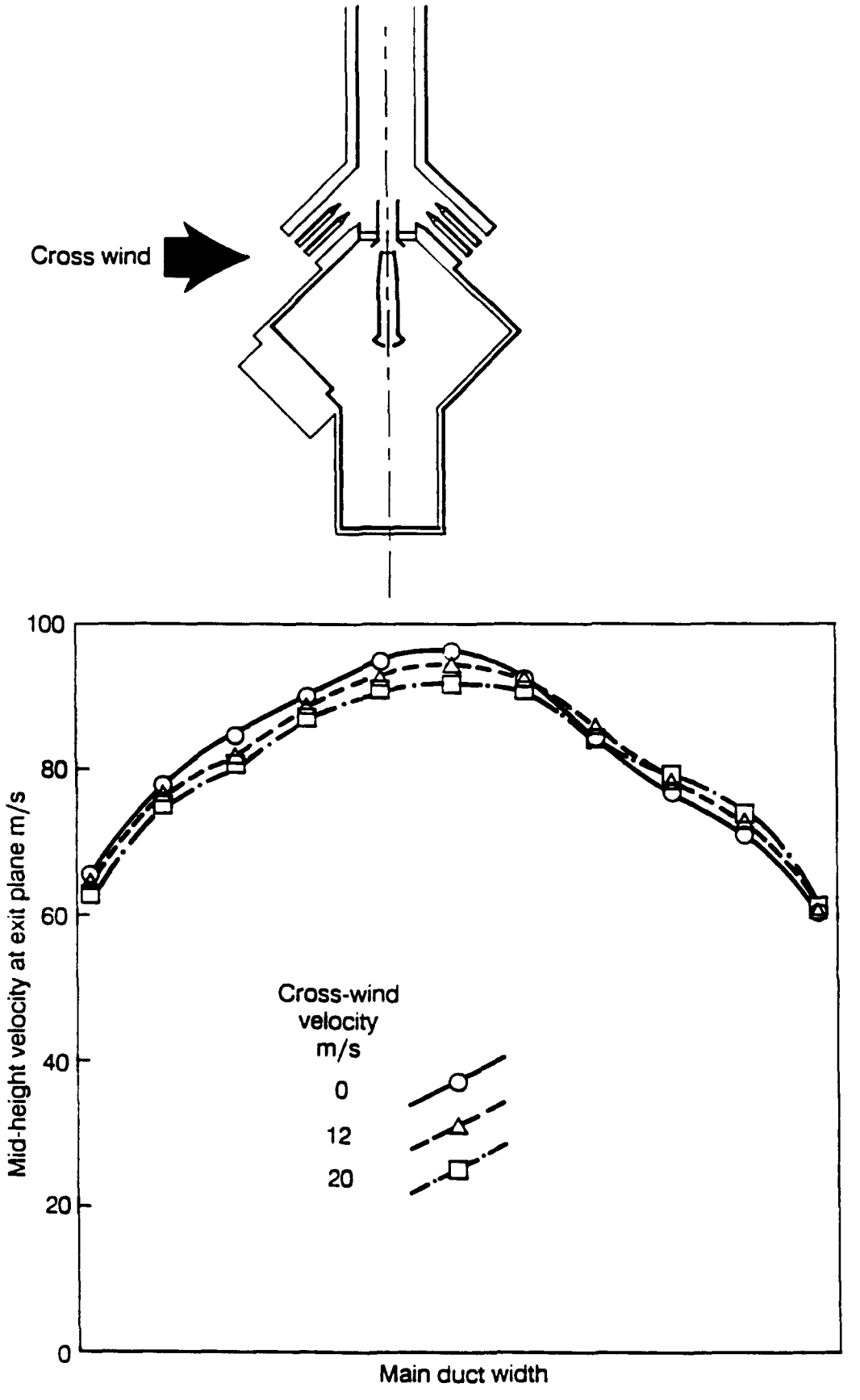


FIGURE 34. EFFECT OF CROSS-WIND ON LATERAL VELOCITY PROFILE - UNINSTALLED ENGINE FACILITY

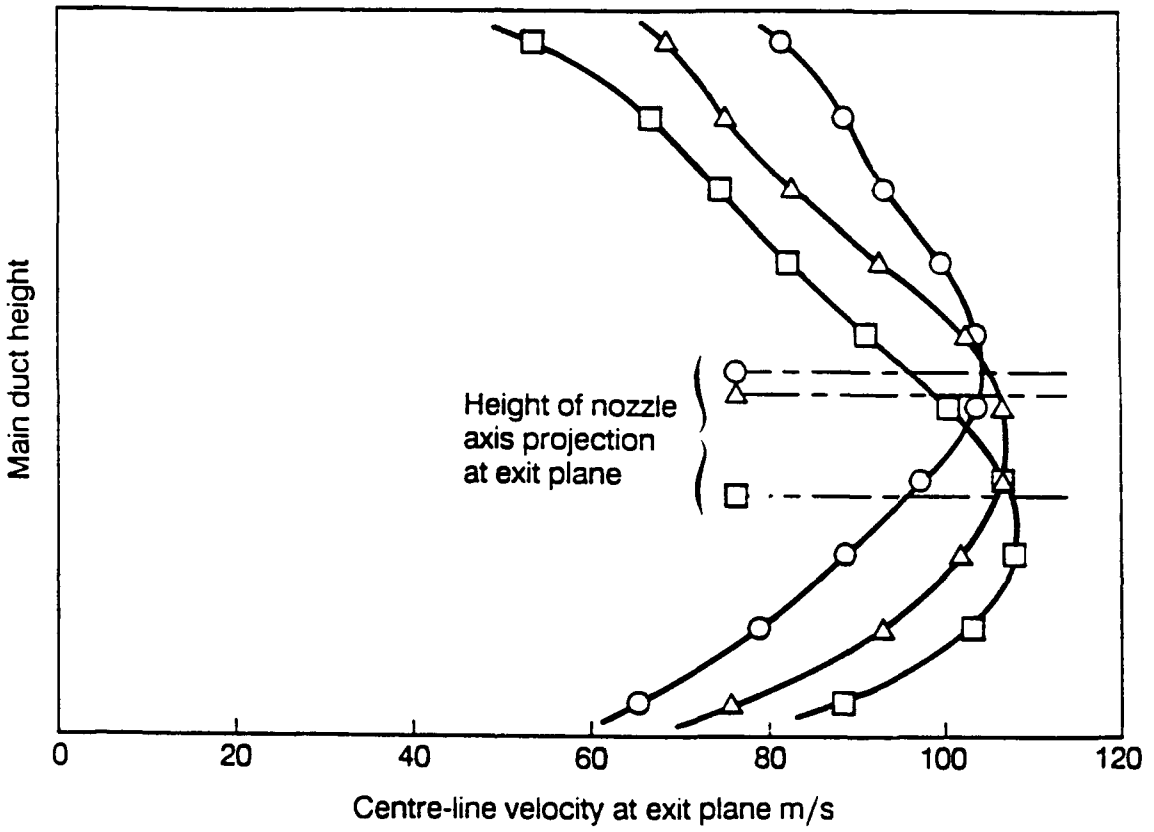


FIGURE 35. EFFECT OF JET MISALIGNMENT ON VERTICAL VELOCITY PROFILE - INSTALLED ENGINE FACILITY

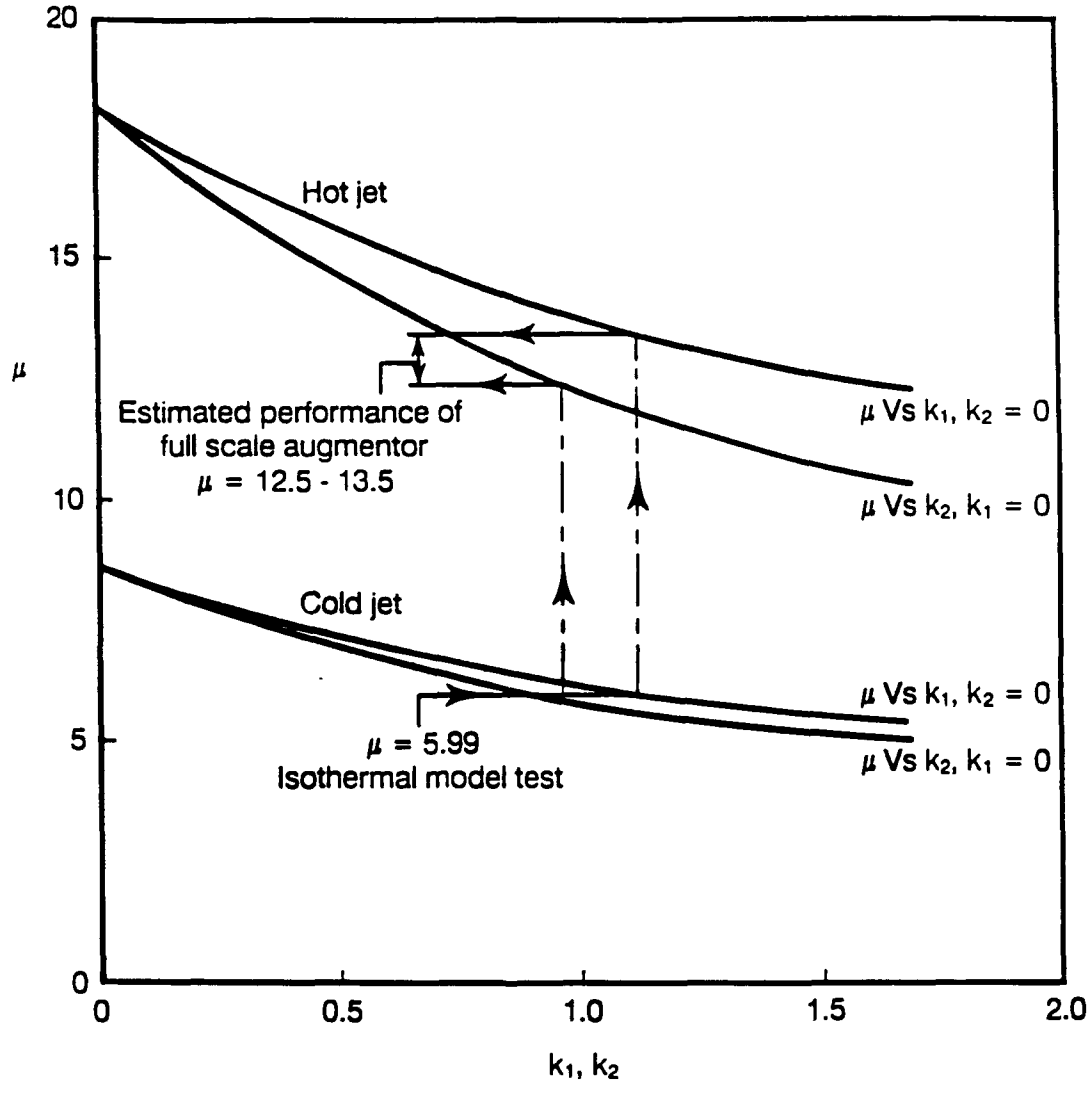


FIGURE 36. ESTIMATION OF FULL SCALE PUMPING PERFORMANCE - INSTALLED ENGINE FACILITY

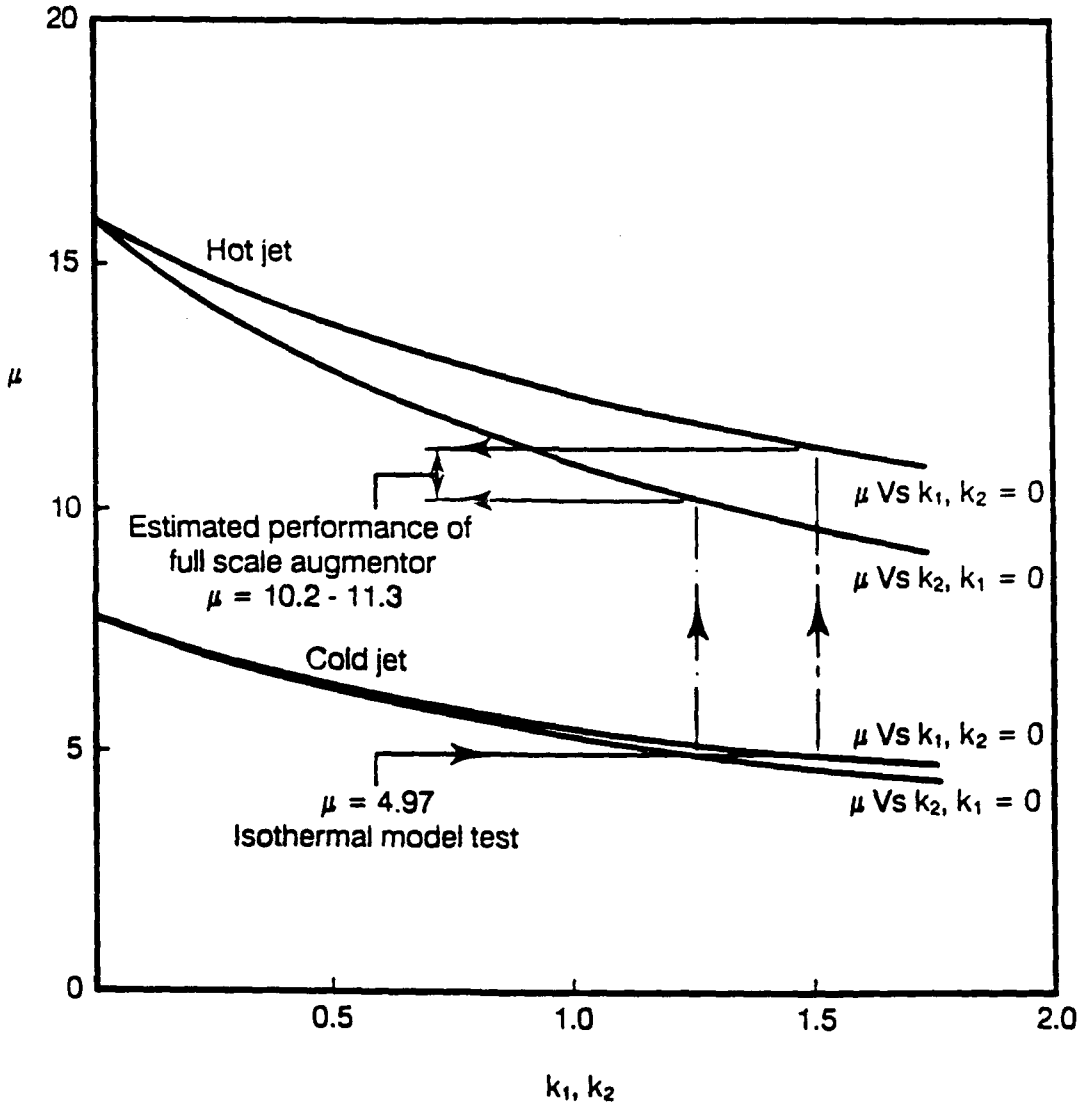


FIGURE 37. ESTIMATION OF FULL SCALE PUMPING PERFORMANCE - UNINSTALLED ENGINE FACILITY

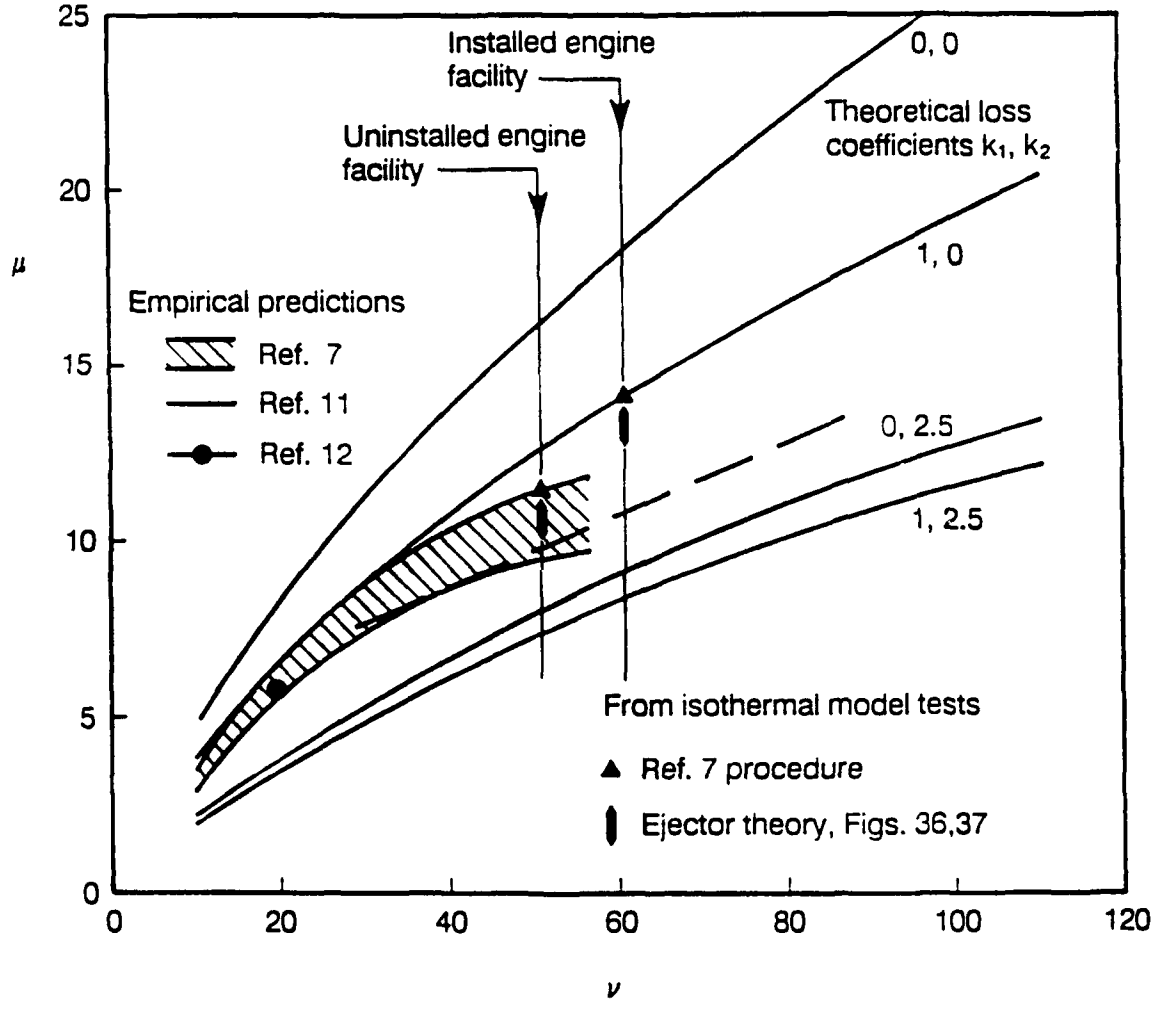


FIGURE 38. AUGMENTOR PUMPING PERFORMANCE - ONE ENGINE AT MAX A/B

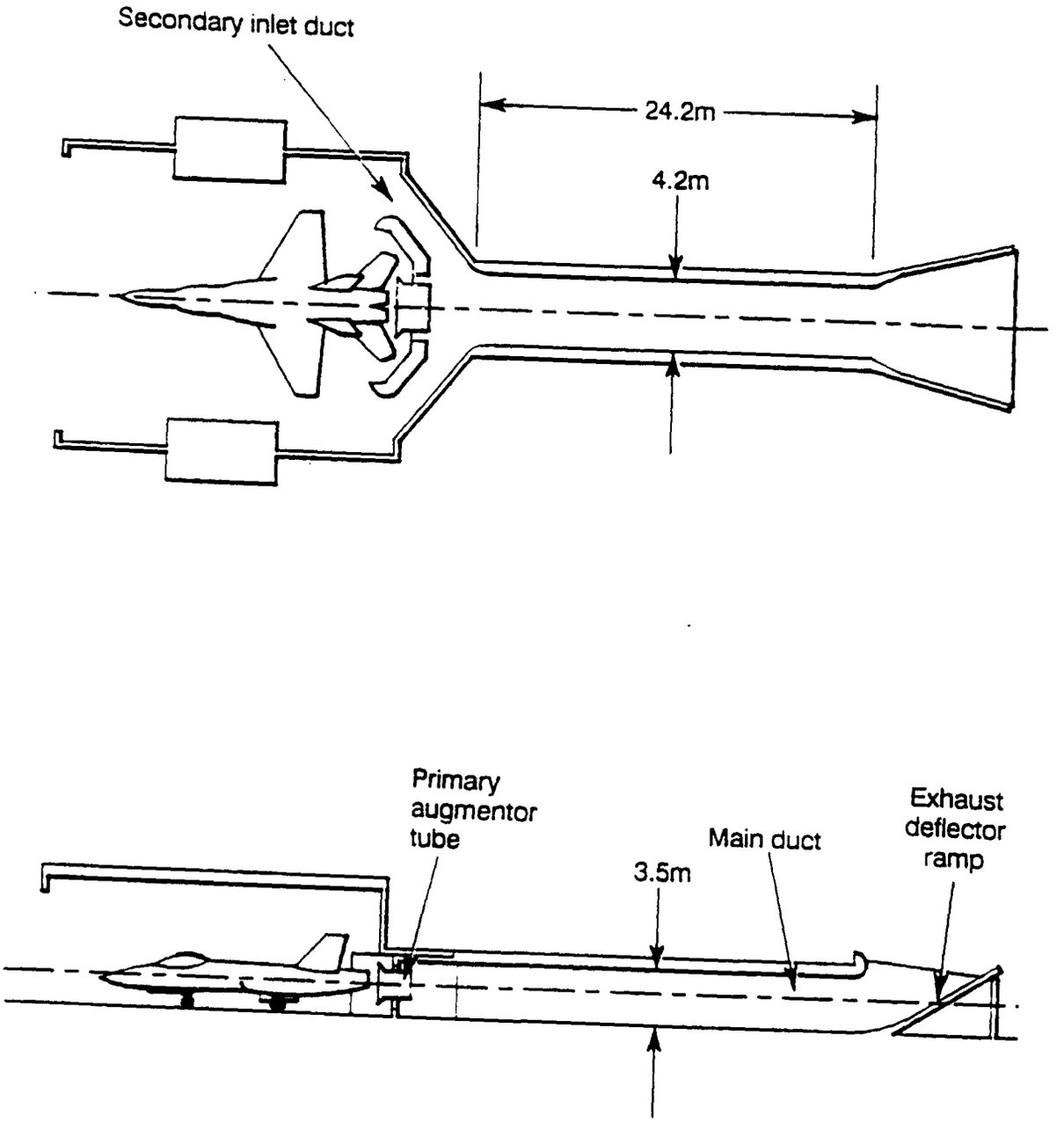


FIGURE 39. INSTALLED ENGINE TEST FACILITY - FINAL DESIGN

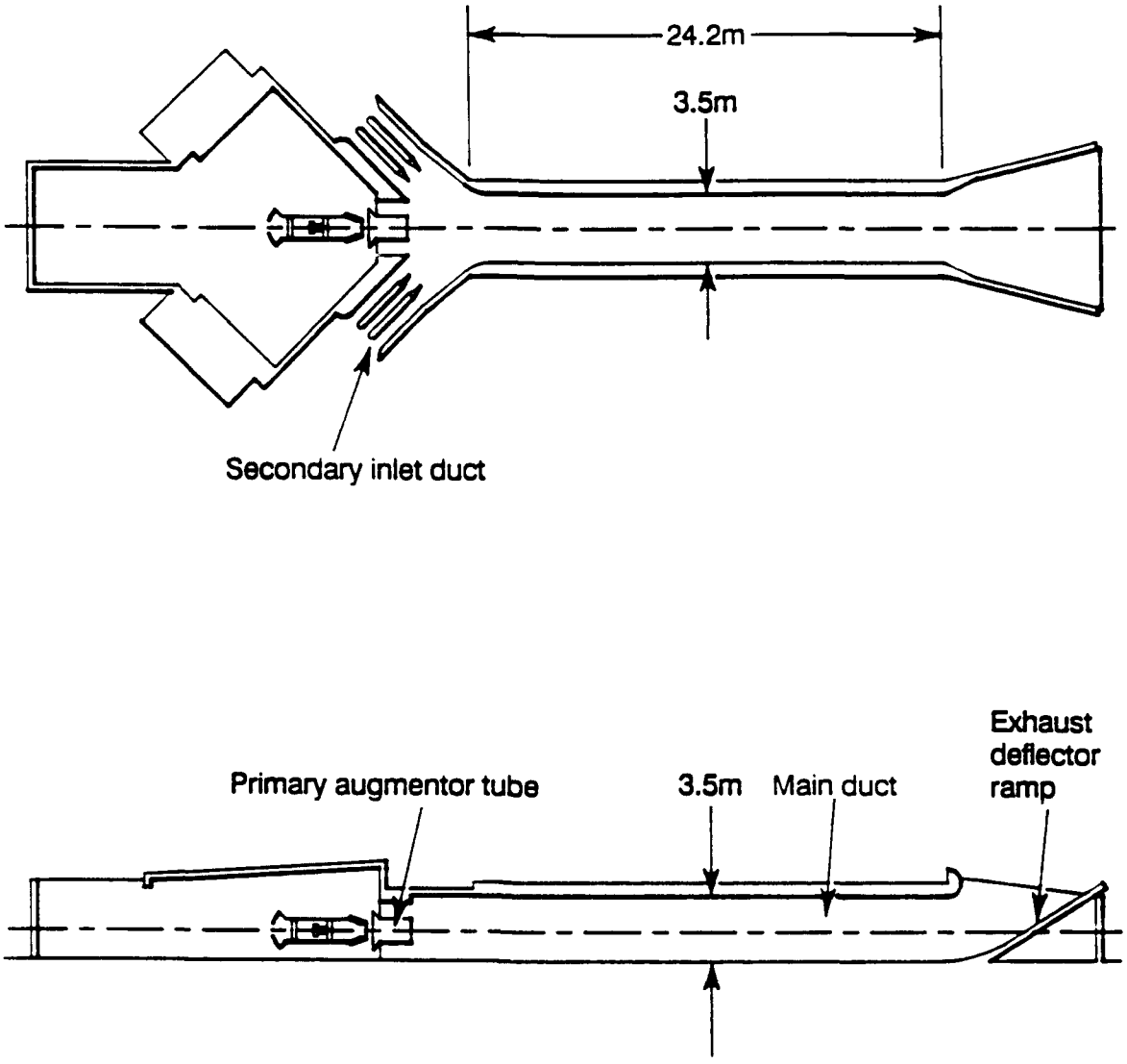


FIGURE 40. UNINSTALLED ENGINE TEST FACILITY - FINAL DESIGN

## DISTRIBUTION

### AUSTRALIA

Department of Defence

Defence Central
- Chief Defence Scientist
- AS, Science Corporate Management (shared copy)
- FAS Science Policy (shared copy)
- Director, Departmental Publications
- Counsellor, Defence Science, London (Doc Data Sheet Only)
- Counsellor, Defence Science, Washington (Doc Data Sheet Only)
- S.A. to Thailand MRD (Doc Data Sheet Only)
- S.A. to the DRC (Kuala Lumpur) (Doc Data Sheet Only)
- OIC TRS, Defence Central Library
- Document Exchange Centre, DSTIC (8 copies)
- Defence Intelligence Organisation
- Librarian H Block, Victoria Barracks, Melbourne
- Director General - Army Development (NSO) (4 copies)
- Defence Industry and Materiel Policy, FAS

Aeronautical Research Laboratory
- Director
- Library
- Chief Flight Mechanics & Propulsion Division
- Branch File - Propulsion
- Authors: Mr S.A. Fisher
  Dr A.M. Abdel-Fattah
- Mr D.E. Glenny

Materials Research Laboratory
- Director/Library

Defence Science & Technology Organisation - Salisbury
- Library

Navy Office
- Navy Scientific Adviser (3 copies Doc Data sheet)
- Aircraft Maintenance and Flight Trials Unit
- RAN Tactical School, Library
- Director Naval Engineering Requirements - Aviation Systems
- Director Aircraft Systems Engineering - Navy
- Superintendent, Aircraft Maintenance and Repair

Army Office
- Scientific Adviser - Army (Doc Data sheet only)
- Engineering Development Establishment, Library
- US Army Research, Development and Standardisation Group

Air Force Office
- Air Force Scientific Adviser
- Aircraft Research and Development Unit
  - Scientific Flight Group
  - Library
- Engineering Branch Library
- Director General Engineering - Air Force
- Director General Facilities - Air Force
- WCE 1 - SQN LDR W. Lear
- AHQ (SMAINTSO)
- HQ Logistics Command (DGLOGENG)

HQ ADF
- Director General Force Development (Air)

Department of Administrative Services
Australian Construction Services
NSW Regional Manager, Project Services

Department of Transport & Communication
Library

Statutory and State Authorities and Industry
L.A. Challis and Associates Pty Ltd
Aero-Space Technologies Australia, Manager/Librarian (2 copies)
Ansett Airlines of Australia, Library
Australian Airlines, Library
Qantas Airways Limited
Civil Aviation Authority
Hawker de Havilland Aust Pty Ltd, Victoria, Library
Hawker de Havilland Aust Pty Ltd, Bankstown, Library
Rolls Royce of Australia Pty Ltd, Manager

Universities and Colleges
Adelaide
Barr Smith Library
Professor Mechanical Engineering

Flinders
Library

LaTrobe
Library

Melbourne
Engineering Library

Monash
Hargrave Library

Newcastle
Library
Professor R. Telfer, Institute of Aviation

New England
Library

Sydney
Engineering Library

NSW
Physical Sciences Library
Head, Mechanical Engineering
Library, Australian Defence Force Academy

Queensland
Library

Tasmania
Engineering Library

Western Australia
Library
Head, Mechanical Engineering

RMIT
Library
Mr M.L. Scott, Aerospace Engineering

University College of the Northern Territory
Library

**BELGIUM**
von Karman Institute for Fluid Mechanics

**CANADA**
CAARC Coordinator Aerodynamics
CAARC Coordinator Propulsion
International Civil Aviation Organization, Library

NRC
Aeronautical & Mechanical Engineering Library
Division of Mechanical Engineering Library
Gas Dynamics Laboratory

Universities and Colleges
Toronto
Institute for Aerospace Studies

**FRANCE**
ONERA

**GERMANY**
Fachinformationszentrum: Energie, Physic, Mathematik GMBH

**INDIA**
CAARC Coordinator Aerodynamics
CAARC Coordinator Propulsion
Defence Ministry, Aero Development Establishment Library
Gas Turbine Research Establishment, Director
Hindustan Aeronautics Ltd, Library
National Aeronautical Laboratory, Information Centre

**ISRAEL**
Technion-Israel Institute of Technology

**ITALY**
Corso Matteotti

**JAPAN**
National Aerospace Laboratory

**NETHERLANDS**
National Aerospace Laboratory (NLR), Library

**NEW ZEALAND**
Defence Scientific Establishment, Library
RNZAF
Transport Ministry, Airworthiness Branch, Library

Universities
Canterbury
Library
Head, Mechanical Engineering

**SWEDEN**
Aeronautical Research Institute, Library
Swedish National Defense Research Institute (FOA)

**SWITZERLAND**
Armament Technology and Procurement Group
F + W (Swiss Federal Aircraft Factory)

**UNITED KINGDOM**

Ministry of Defence, Research, Materials and Collaboration
CAARC, Secretary
CAARC Coordinator Aerodynamics
Royal Aircraft Establishment
Bedford, Library
Pyestock, Director
CAARC Coordinator, Propulsion
Aircraft Research Association, Library
Rolls-Royce Ltd, Aero Division Bristol, Library
British Aerospace
Kingston-upon-Thames, Library
Hatfield-Chester Division, Library
Short Brothers Ltd, Technical Library

Universities and Colleges

Bristol
Engineering Library

Cambridge
Library, Engineering Department
Whittle Library

London
Head, Aero Engineering

Manchester
Head, Dept of Engineering (Aeronautical)

Nottingham
Science Library

Southampton
Library

Liverpool
Head, Fluid Mechanics Division

Strathclyde
Library

Cranfield Inst. of Technology
Library

Imperial College
Aeronautics Library

**UNITED STATES OF AMERICA**

NASA Scientific and Technical Information Facility
Boeing Commercial Airplanes
United Technologies Corporation, Library
Lockheed-California Company
Lockheed Georgia
McDonnell Aircraft Company, Library

SPARES (10 COPIES)

TOTAL (143 COPIES)

AL 149 DEPARTMENT OF DEFENCE

# DOCUMENT CONTROL DATA

PAGE CLASSIFICATION
UNCLASSIFIED

PRIVACY MARKING

| 1a. AR NUMBER | 1b. ESTABLISHMENT NUMBER | 2. DOCUMENT DATE | 3. TASK NUMBER |
|---|---|---|---|
| AR-006-126 | ARL-PROP-R-177 | OCTOBER 1990 | AIR 99/040 |

4. TITLE
AEROTHERMODYNAMIC DESIGN APPRAISAL OF NOISE SUPPRESSORS FOR F/A-18 ENGINE RUN-UP FACILITIES AT RAAF WILLIAMTOWN

5. SECURITY CLASSIFICATION (PLACE APPROPRIATE CLASSIFICATION IN BOX(S) IE. SECRET (S), CONF. (C) RESTRICTED (R), UNCLASSIFIED (U) ).

| DOCUMENT | TITLE | ABSTRACT |
|---|---|---|
| U | U | U |

6. NO. PAGES
62

7. NO. REFS.
16

8. AUTHOR(S)
S.A. Fisher
A.M. Abdel-Fattah

9. DOWNGRADING/DELIMITING INSTRUCTIONS
Not applicable

10. CORPORATE AUTHOR AND ADDRESS
AERONAUTICAL RESEARCH LABORATORY
506 LORIMER STREET
FISHERMENS BEND VIC 3207

11. OFFICE/POSITION RESPONSIBLE FOR:
SPONSOR RAAF
SECURITY -
DOWNGRADING -
APPROVAL DARL

12. SECONDARY DISTRIBUTION (OF THIS DOCUMENT)
Approved for public release.

OVERSEAS ENQUIRIES OUTSIDE STATED LIMITATIONS SHOULD BE REFERRED THROUGH DSTIC, ADMINISTRATIVE SERVICES BRANCH, DEPARTMENT OF DEFENCE, ANZAC PARK WEST OFFICES, ACT 2601

13a. THIS DOCUMENT MAY BE ANNOUNCED IN CATALOGUES AND AWARENESS SERVICES AVAILABLE TO ....
No limitations

13b. CITATION FOR OTHER PURPOSES (IE. CASUAL ANNOUNCEMENT) MAY BE [X] UNRESTRICTED OR [ ] AS FOR 13a.

14. DESCRIPTORS

| | | 15. DISCAT SUBJECT CATEGORIES |
|---|---|---|
| Exhaust systems | | 2105 |
| Engine tests | Noise reduction | 010101 |
| F/A-18 aircraft | Exhaust systems | 2402 |
| Jet engine noise | Aerodynamic characteristics | |
| Jet engine exhaust | F404 engines | |

16. ABSTRACT

*Upgraded facilities for ground running of F404 engines in F/A-18 aircraft at RAAF Williamtown will feature air-cooled exhaust augmentors for noise suppression. Aerothermodynamic aspects of the augmentor designs were appraised in some detail, making use of isothermal scale model tests, ejector theory and available empirical data.*

*In initial design development, quantitative assessments were made of cooling flow pumping performance. Changes were recommended to improve the aerodynamic characteristics of the exhaust augmentors and eliminate high risk features, and the sizes of the augmentor ducts were significantly reduced. The model tests identified certain geometric features which were important for symmetry of the flow in the augmentor ducts and to pumping performance.Once modified accordingly, the designs displayed satisfactory aerodynamic behaviour,which was tolerant to both inlet asymmetries and reasonable levels of engine jet misalignment. The pumping performance was shown to exceed the design requirements.*

| PAGE CLASSIFICATION |
| --- |
| UNCLASSIFIED |
| PRIVACY MARKING |

THIS PAGE IS TO BE USED TO RECORD INFORMATION WHICH IS REQUIRED BY THE ESTABLISHMENT FOR ITS OWN USE BUT WHICH WILL NOT BE ADDED TO THE DISTIS DATA UNLESS SPECIFICALLY REQUESTED.

16. ABSTRACT (CONT).

17. IMPRINT

**AERONAUTICAL RESEARCH LABORATORY, MELBOURNE**

| 18. DOCUMENT SERIES AND NUMBER | 19. COST CODE | 20. TYPE OF REPORT AND PERIOD COVERED |
| --- | --- | --- |
| Propulsion Report 177 | 42 4380 | |

21. COMPUTER PROGRAMS USED

22. ESTABLISHMENT FILE REF.(S)

C2/199

23. ADDITIONAL INFORMATION (AS REQUIRED)